Genetics and Evolution of Hybrid Male Sterility in House Mice

Michael A. White,[1] Maria Stubbings, Beth L. Dumont,[2] and Bret A. Payseur[3]
Laboratory of Genetics, University of Wisconsin, Madison, Wisconsin 53706

ABSTRACT Comparative genetic mapping provides insights into the evolution of the reproductive barriers that separate closely related species. This approach has been used to document the accumulation of reproductive incompatibilities over time, but has only been applied to a few taxa. House mice offer a powerful system to reconstruct the evolution of reproductive isolation between multiple subspecies pairs. However, studies of the primary reproductive barrier in house mice—hybrid male sterility—have been restricted to a single subspecies pair: *Mus musculus musculus* and *Mus musculus domesticus*. To provide a more complete characterization of reproductive isolation in house mice, we conducted an F_2 intercross between wild-derived inbred strains from *Mus musculus castaneus* and *M. m. domesticus*. We identified autosomal and X-linked QTL associated with a range of hybrid male sterility phenotypes, including testis weight, sperm density, and sperm morphology. The pseudoautosomal region (PAR) was strongly associated with hybrid sterility phenotypes when heterozygous. We compared QTL found in this cross with QTL identified in a previous F_2 intercross between *M. m. musculus* and *M. m. domesticus* and found three shared autosomal QTL. Most QTL were not shared, demonstrating that the genetic basis of hybrid male sterility largely differs between these closely related subspecies pairs. These results lay the groundwork for identifying genes responsible for the early stages of speciation in house mice.

THE genetic dissection of reproductive barriers between species is a powerful approach to understanding speciation. In some cases, genetic mapping has revealed the identities and functions of the gene networks responsible for reproductive isolation (Sawamura and Yamamoto 1997; Ting *et al.* 1998; Barbash *et al.* 2003; Presgraves *et al.* 2003; Brideau *et al.* 2006; Bayes and Malik 2009; Ferree and Barbash 2009; Mihola *et al.* 2009; Phadnis and Orr 2009; Tang and Presgraves 2009). By providing a list of genomic locations that contribute to reproductive barriers, mapping also allows investigation of the role of genomic context, including local recombination rate (Noor *et al.* 2001; Rieseberg 2001; Butlin 2005; Nachman and Payseur 2012), in speciation. Phenotypes associated with reproductive isolation have been mapped in a variety of species, with an emphasis on hybrid sterility and hybrid inviability (Hollocher and Wu 1996; True *et al.* 1996; Tao *et al.* 2003; Sweigart *et al.* 2006; Bomblies *et al.* 2007; Masly and Presgraves 2007; Moyle 2007; Chen *et al.* 2008; Lee *et al.* 2008; Long *et al.* 2008; Kao *et al.* 2010; Martin and Willis 2010).

The comparison of reproductive isolation among species pairs has revealed general patterns that characterize speciation. For example, hybrid sterility tends to evolve before hybrid inviability (Coyne and Orr 1989). A worthwhile extension of this comparative framework focuses on the loci responsible for reproductive barriers (Moyle and Payseur 2009). By comparing loci mapped in different species pairs, genetic changes that increase reproductive isolation can be assigned to specific phylogenetic lineages, revealing the evolutionary history of reproductive barriers (Moyle and Nakazato 2008). This information enables the evaluation of models that describe the accumulation of reproductive isolating mutations (Orr 1995), the distinction between classes of incompatibilities (*e.g.*, "derived-derived" and "ancestral-derived"; Orr 1995; Cattani and Presgraves 2009), and the temporal ordering of genetic changes that contribute to different reproductive barriers.

Recent applications of this comparative genetics approach have produced new insights into the evolution of reproductive isolation. Overlapping quantitative trait loci

doi: 10.1534/genetics.112.140251
Manuscript received March 3, 2012; accepted for publication April 23, 2012
Supporting information is available online at http://www.genetics.org/content/suppl/2012/05/02/genetics.112.140251.DC1.
[1]Present address: Division of Human Biology, Fred Hutchinson Cancer Research Center, Seattle, WA 98109.
[2]Present address: Department of Genome Sciences, University of Washington, Seattle, WA 98195.
[3]Corresponding author: 2428 Genetics/Biotech, Laboratory of Genetics, University of Wisconsin, Madison, WI 53706. E-mail: payseur@wisc.edu

(QTL) control hybrid pollen/seed sterility in two species pairs of Solanum, suggesting common evolutionary origins for the underlying mutations (Moyle and Graham 2005; Moyle and Nakazato 2008). The number of incompatibilities involved in hybrid dysfunction may increase faster than linearly with divergence time in Drosophila (Matute *et al.* 2010; but see Barbash 2011) and in Solanum (Moyle and Nakazato 2010), as predicted by theory assuming the Dobzhansky–Muller model (Orr 1995; Turelli and Orr 2000; Orr and Turelli 2001). Additional comparative genetic studies are needed, especially for recently diverged species where genetic factors closely tied to speciation can be identified.

House mice provide a powerful system for understanding the evolution of reproductive isolation during the early stages of speciation. The clade is composed of three closely related subspecies (*Mus musculus musculus*, *Mus musculus domesticus*, and *Mus musculus castaneus*), which rapidly diverged from a common ancestor only 500,000 generations ago (She *et al.* 1990; Boursot *et al.* 1996; Suzuki *et al.* 2004; Salcedo *et al.* 2007; Geraldes *et al.* 2008). The geographic ranges of these subspecies extend throughout the Mediterranean and Western Europe (*M. m. domesticus*), Eastern Europe and Northern Asia (*M. m. musculus*), and Southern Asia (*M. m. castaneus*) (Boursot *et al.* 1993). The best-studied region of geographical overlap is in central Europe, where *M. m. musculus* and *M. m. domesticus* hybridize in a zone of secondary contact (Boursot *et al.* 1993; Sage *et al.* 1993). Patterns of gene flow in this hybrid zone and reproductive characteristics in hybrid mice indicate that *M. m. musculus* and *M. m. domesticus* are partially reproductively isolated. Diagnostic loci show steep allele frequency clines across the hybrid zone (Vanlerberghe *et al.* 1986; Dod *et al.* 1993, 2005; Munclinger *et al.* 2002; Payseur *et al.* 2004; Payseur and Nachman 2005; Raufaste *et al.* 2005; Macholán *et al.* 2007, 2008; Teeter *et al.* 2008, 2010), suggesting that multiple genomic regions confer reproductive barriers (Payseur 2010). Hybrid males from this zone (Turner *et al.* 2012) and from the laboratory (Iványi *et al.* 1969; Forejt and Iványi 1974; Storchová *et al.* 2004; Britton-Davidian *et al.* 2005; Vyskočilová *et al.* 2005, 2009; Good *et al.* 2008a,b) exhibit reproductive phenotypes that indicate subfertility or sterility. Hybrid male sterility has been linked to loci on the X chromosome (Oka *et al.* 2004; Storchová *et al.* 2004; Britton-Davidian *et al.* 2005; Good *et al.* 2008a,b and 2010 Vyskočilová *et al.* 2009) and the autosomes (Forejt and Iványi 1974; Forejt 1996; Oka *et al.* 2007; Gregorová *et al.* 2008; Mihola *et al.* 2009). The only known vertebrate hybrid sterility gene, *Prdm9*, was found in crosses between these two subspecies (Forejt and Iványi 1974; Forejt 1996; Mihola *et al.* 2009). Female hybrid sterility (Britton-Davidian *et al.* 2005), reduced immunological function in hybrids (Sage *et al.* 1986; Moulia *et al.* 1991), faster fertilization rates of conspecific sperm (Dean and Nachman 2009), and female mating preferences for conspecific males (Laukaitis *et al.* 1997) provide additional reproductive barriers between these subspecies.

Reproductive barriers between *M. m. domesticus* and *M. m. castaneus* have not been directly evaluated, but some evidence suggests that isolation may be less severe than that between *M. m. musculus* and *M. m. domesticus*. In natural populations, hybridization has occurred between the two subspecies in human-mediated zones of secondary contact (Orth *et al.* 1998). Hybridization may have also occurred in Iran during subspecies range expansion (Duvaux *et al.* 2011). Patterns of genetic differentiation indicate higher levels of introgression from *M. m. domesticus* into *M. m. castaneus* than between *M. m. musculus* and *M. m. domesticus* (Geraldes *et al.* 2008, 2011). Inbred strains of *M. m. castaneus* have been repeatedly crossed to classical inbred strains of house mice (mostly of *M. m. domesticus* origin) to map phenotypes (*e.g.*, Janaswami *et al.* 1997; Anunciado *et al.* 2000; Ishikawa *et al.* 2000; Lyons *et al.* 2003, 2004; Yi *et al.* 2006). Mapping populations usually have been established using backcross and intercross designs, suggesting that F_1 hybrids between these two subspecies are effectively fertile. However, the unusual history of the classical strains, which includes hybridization between different subspecies (Beck *et al.* 2000; Frazer *et al.* 2007; Yang *et al.* 2007; Keane *et al.* 2011), might have shaped these patterns. Additionally, even if F_1 hybrid sterility does not block reproduction between *M. m. castaneus* and *M. m. domesticus*, barriers could appear in subsequent generations. Recessive-recessive incompatibilities that isolate these subspecies would not be visible in F_1's. Such incompatibilities contribute to hybrid dysfunction in other taxa (Presgraves 2003; Oka *et al.* 2004; White *et al.* 2011) and are predicted to be more common than other types of disrupted interactions (Muller 1942). Support for the existence of recessive-recessive incompatibilities in crosses involving *M. m. castaneus* and *M. m. domesticus* comes from the identification of multiple genomic regions in *M. m. castaneus* that reduce fertility only when homozygous. Several independent segments of the *M. m. castaneus* (CAST/EiJ strain) genome caused reduced fecundity when introgressed on to the genomic background of a strain primarily descended from *M. m. domesticus* (Davis *et al.* 2007).

Here, we provide the first detailed characterization of the genetic architecture of hybrid male sterility between *M. m. castaneus* and *M. m. domesticus*. We report QTL for a broad range of male fertility traits in the F_2 generation. We compare these QTL to those discovered in an equivalent study of hybrid male sterility between *M. m. domesticus* and *M. m. musculus* (White *et al.* 2011) to understand the evolution of reproductive isolation in house mice.

Materials and Methods

Animal husbandry and crossing design

Two wild-derived inbred strains purchased from Jackson Laboratories (www.jax.org) were used to conduct the intercrosses: *M. m. castaneus* (CAST/EiJ) and *M. m. domesticus*

(WSB/EiJ). Parents were crossed in reciprocal directions to generate the F_1 hybrids (*M. m. castaneus*^{CAST} × *M. m. domesticus*^{WSB} and *M. m. domesticus*^{WSB} × *M. m. castaneus*^{CAST}). The F_2 intercross was generated by crossing F_1 siblings from both parental directions: (*M. m. castaneus*^{CAST} × *M. m. domesticus*^{WSB}) F_1 × (*M. m. castaneus*^{CAST} × *M. m. domesticus*^{WSB}) F_1 and (*M. m. domesticus*^{WSB} × *M. m. castaneus*^{CAST}) F_1 × (*M. m. domesticus*^{WSB} × *M. m. castaneus*^{CAST}) F_1. All crosses occurred within the University of Wisconsin School of Medicine and Public Health mouse facility according to animal care protocols approved by the University of Wisconsin Animal Care and Use Committee. Mice were provided with food and water *ad libitum*. Pups were weaned into same-sex sibling groups at 21 days and males were separated into individual cages at ~56 days. Males were killed for phenotyping at 70 days of age (±5 days) using carbon dioxide.

Quantification of male fertility phenotypes

Five morphological characters were quantified to diagnose subfertility and sterility in males: testis weight (Iványi *et al.* 1969; Forejt and Iványi 1974), sperm density (Searle and Beechey 1974; Storchová *et al.* 2004; Vyskočilová *et al.* 2005), proportion of abnormal sperm (Kawai *et al.* 2006), sperm head morphology (Oka *et al.* 2004; Storchová *et al.* 2004; Kawai *et al.* 2006), and stage VII seminiferous tubule area. Variation in these phenotypes will stem from two sources: strain-specific differences in fertility characteristics and hybrid incompatibilities that are not present in the parent strains. Testes were weighed fresh immediately upon dissection, fixed overnight in Bouin's, and washed in an ethanol series. The right testis was embedded in paraffin, sectioned at 6 μm, and stained with hematoxylin and eosin following standard procedures. Testis weight was positively correlated with body weight in F_2 males (Pearson's $r = 0.255$, $P < 0.001$). To account for this correlation, testis weight was divided by body weight prior to QTL analyses. We also mapped QTL for absolute right testis weight and for the residual trait scores of testis weight regressed on body weight. Sperm was extracted from the left and right cauda epididymides to measure sperm density, sperm head morphology, and abnormal sperm type as previously outlined (White *et al.* 2011). Cross-sectional seminiferous tubule area was only quantified in stage VII tubules to control for variance in area among the different stages of spermatogenesis (Russell *et al.* 1990) as previously described (White *et al.* 2011). The area of seminiferous tubules was positively correlated with testis weight (Pearson's $r = 0.407$, $P < 0.001$). To account for this correlation, all QTL analyses were conducted using the residual trait scores from a least squares regression of seminiferous tubule area on testis weight.

To quantify X and Y chromosome synapsis, Dumont and Payseur (2011) collected early meiotic cells for CAST/EiJ, WSB/EiJ, and F_1 hybrids. X and Y chromosome synapsis was recorded as a binary indicator for each cell in late pachytene. Synapsis was defined by the formation of a synaptonemal complex between the pseudoautosomal regions of the two chromosomes, as revealed by the merger of SYCP3 signals across the pseudoautosomal region (PAR). Within each parental strain and F_1, cells were pooled across multiple males [CAST/EiJ: three males, 91 total cells; WSB/EiJ: five males, 99 total cells; (CAST/EiJ × WSB/EiJ) F_1: four males, 96 total cells; and (WSB/EiJ × CAST/EiJ) F_1: one male, 63 total cells]. The proportion of X and Y chromosomes that were not synapsed was calculated across the total pool of cells.

Genotyping and quality control procedures

Genomic DNA extraction, SNP design, genotyping, and quality control procedures, were conducted as previously described (White *et al.* 2011). After quality control, there were 188 SNPs across the autosomes and X chromosome, one Y-linked SNP, one mitochondrial SNP, and two SNPs within the *M. m. castaneus* PAR. Pairwise genotypic similarity of males fell between 13.8 and 85.8% with the exception of two males who were identical at >98.9% of their markers. These males likely reflected duplicate DNA samples and were removed from the analysis. After quality control, the final data set retained 313 males. Only 4.9% of markers were missing from the entire data matrix. All genotypes within the PAR were verified by amplifying ~1 kb across the SNPs with polymerase chain reaction (PCR) and Sanger sequencing the PCR fragment.

QTL analyses

The genetic map was estimated from a total of 579 males and females with the *est.map* function of R/qtl (Broman *et al.* 2003; Broman and Sen 2009), using a Carter–Falconer mapping function (Carter and Falconer 1951; Broman *et al.* 2002). Because the stringent filtering scheme for markers ensured few genotyping errors (Dumont *et al.* 2011), the map was estimated assuming a genotyping error rate of zero. SNPs were spaced at an average distance of 8.06 cM. Marker order matched that of the reference mouse genome (Mouse Genome Sequencing Consortium 2002), suggesting no large chromosomal rearrangements. Physical positions were interpolated using the physical and genetic map positions of flanking markers. Crossing design, the number of males, and the number of SNPs were nearly identical to a previous study between *M. m. musculus* and *M. m. domesticus* (White *et al.* 2011). This enabled a direct comparison of the genetic architecture of hybrid male sterility.

Interval mapping was conducted using the *scanone* function in R/qtl (Lander and Botstein 1989; Broman and Sen 2009) as previously described (White *et al.* 2011). Genotype probabilities were calculated between markers every 2 cM using a genotyping error rate of 0.001. Phenotypes were mapped using standard interval mapping except for the abnormal sperm types, which were mapped using the extended Haley–Knott method (Feenstra *et al.* 2006).

Joint analyses of multiple QTL were conducted with two-dimensional, two-QTL scans and multiple QTL modeling as previously described (White *et al.* 2011). All phenotypes

Table 1 Mean fertility traits for parents and F_1's

Phenotype	*M. m. cast*[a]	*M. m. dom.*[a]	*cast. X dom.*[a]	*dom. X cast.*[a]
Right testis weight (mg)	43.15[b] (5; ±1.49)	66.36[c] (19; ±11.51)	63.40[c] (22; ±4.011)	78.70[d] (13; ±6.47)
Relative right testis weight (mg/g)	3.11[b] (5; ±0.19)	3.95[c] (19; ±0.57)	3.86[c] (22; ±0.29)	3.45[d] (13; ±0.28)
Sperm density (millions/mL)	3.089[e] (25; ±0.82)	12.37[f] (17; ±4.08)	15.24[f] (22; ±3.07)	14.68[f] (11; ±4.70)
Seminiferous tubule area (μm^2)	25,690.47[b] (5; ±1725.04)	34,583.45[c] (6; ±5328.86)	24,917.02[b] (6; ±2269.43)	26,496.08[b] (6; ±2460.66)
Proportion of apoptotic cells[g]	0[e] (5; ±0.000)	0.002[e] (6; ±0.003)	0.048[f] (6; ±0.016)	0.065[f] (6; ±0.018)
Proximal bent tail[h]	0.069[e] (8; ±0.030)	0.042[e] (10; ±0.022)	0.0090[f] (10; ±0.0074)	0.0060[f] (10; 0.0070)
Distal bent tail[h]	0.020[e] (8; ±0.011)	0.011[e,f] (10; ±0.012)	0.0020[f] (10; ±0.0042)	0.0040[f] (10; ±0.0052)
Headless/tailless sperm[h]	0.18[e] (8; ±0.060)	0.072[f] (10; ±0.036)	0.092[f] (10; ±0.041)	0.081[f] (10; ±0.037)
Amorphous sperm head[h]	0.19[e] (8; ±0.086)	0.013[f] (10; ±0.013)	0.0090[f] (10; ±0.012)	0.0050[f] (10; ±0.0097)
Total sperm abnormalities[h]	0.46[e] (8; ±0.071)	0.14[f] (10; ±0.052)	0.11[f] (10; ±0.044)	0.096[f] (10; ±0.039)
Unpaired X/Y chromosomes[i]	0.066[j] (91)	0.051[j] (99)	0.375[k] (96)	0.302[k] (63)

[a] Mean (*N*; SD). Unpaired X/Y chromosomes, proportion (total cells).
[b,c,d] Groups significantly different by *t*-test, $P < 0.05$.
[e,f] Groups significantly different by Mann-Whitney U Test, $P < 0.05$.
[g] Proportion of seminiferous tubules with any apoptotic cells.
[h] Proportion of abnormal sperm.
[i] Proportion of meiocytes with unpaired X and Y chromosomes at late pachytene.
[j,k] Groups significantly different by logistic regression, $P < 0.001$.

were mapped using standard interval mapping, with the exception of amorphous sperm heads, which was mapped using Haley–Knott regression (Haley and Knott 1992). Multiple QTL models were fitted with the *stepwiseqtl* function of R/qtl (Manichaikul *et al.* 2009; Arends *et al.* 2010). In models that included the mitochondrion or Y chromosome, a covariate that accounted for the intercross direction was added. This covariate was used to capture the phenotypic effects from the mitochondrion or Y chromosome. A penalized LOD score derived from the 10,000 *scantwo* permutations was used to compare models. Genotype probabilities were calculated every 3 cM with a genotyping error rate of 0.001 and all phenotypes were mapped using Haley–Knott regression (Haley and Knott 1992).

Results

Parental and F_1 hybrid fertility

Most phenotypes indicated that *M. m. castaneus*^{CAST} males were less fertile than *M. m. domesticus*^{WSB} males. There was no significant difference between *M. m. castaneus*^{CAST} and *M. m. domesticus*^{WSB} for proximal bent tail frequency or distal bent tail frequency, but *M. m. castaneus*^{CAST} displayed significantly higher levels of infertility for all other phenotypes (Table 1). Furthermore, *M. m. castaneus*^{CAST} displayed sperm heads with reduced apical hooks, consistent with subfertility (Figure 1A). To begin to determine whether these differences were strain-specific, we conducted a preliminary examination of another strain of *M. m. castaneus* (CIM). *M. m. castaneus*^{CIM} showed relative right testis weights well below those of *M. m. castaneus*^{CAST} (*M. m. castaneus*^{CAST}, 3.11; *M. m. castaneus*^{CIM}, 1.94; *t*-test: $P < 0.001$), indicating that the reduced fertility measures of *M. m. castaneus*^{CAST} were not unique to this strain. Although *M. m. castaneus*^{CAST} exhibited some degree of subfertility, males paired with *M. m. domesticus*^{WSB} females produced offspring.

F_1 hybrid male sterility between *M. m. castaneus*^{CAST} and wild-derived strains from other subspecies of house mice has not been evaluated. We quantified sterility phenotypes in F_1 hybrid males from reciprocal crosses between *M. m. castaneus*^{CAST} and *M. m. domesticus*^{WSB}. For most phenotypes examined, males from both directions of the cross had fertility measures that matched or exceeded those of *M. m. domesticus*^{WSB} males (Table 1). Like the *M. m. domesticus*^{WSB} parent, F_1's from both cross directions also showed sperm heads with pronounced apical hooks (Figure 1A), a shape consistent with fertility (White *et al.* 2011), and low frequencies of abnormal sperm types (Table 1). Although F_1's generally showed high levels of fertility, several potential signs of hybrid subfertility emerged. The (*M. m. domesticus*^{WSB} × *M. m. castaneus*^{CAST}) F_1 had significantly reduced relative right testis weights compared to *M. m. domesticus*^{WSB} and the reciprocal F_1 (Table 1). In addition, F_1's from both cross directions had significantly reduced seminiferous tubule areas (indistinguishable from the *M. m. castaneus*^{CAST} parent; Table 1). Both F_1 directions also had a higher percentage of seminiferous tubules with apoptotic cells than either parent (Table 1). Hybrid defects in spermatogenesis were also apparent in spermatocytes in the late phase of meiosis. We detected significantly higher proportions of spermatocytes with unpaired X and Y chromosomes as compared to either parent strain (Table 1).

We set up intercrosses by pairing F_1 males with F_1 females from the same parental cross direction. Males from both F_1 directions sired offspring in every pairing attempted [(*M. m. domesticus*^{WSB} × *M. m. castaneus*^{CAST}) F_1 direction: 4 pairings; (*M. m. castaneus*^{CAST} × *M. m. domesticus*^{WSB}) F_1 direction: 10 pairings], indicating that males in both cross directions were fertile. Although we detected a few F_1 phenotypes that revealed defects during spermatogenesis, they had no strong effect on the ability to sire offspring.

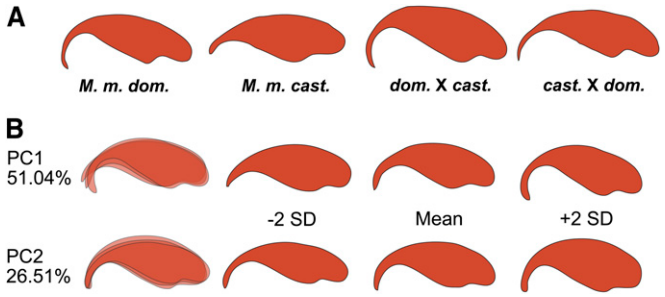

Figure 1 Epididymal sperm head morphologies. *M. m. domesticus*^{WSB}, *M. m. castaneus*^{CAST}, and the F_1 hybrids (A). Epididymal sperm head morphology was characterized by two main principal components in the F_2 males (B). The first principal component largely explained changes in the apical hook, whereas the second principal component characterized a change in sperm head width.

F_2 hybrid sterility

We examined hybrid male sterility in 313 F_2 males (99 males originated from the direction with *M. m. domesticus*^{WSB} as the female parent; 214 males originated from the direction with *M. m. castaneus*^{CAST} as the female parent). There was an expansion of variance for all phenotypes examined in the F_2 males (Figure 2), with a large proportion of the distributions falling in a low fertility range. We used phenotypic means from the sterile F_1 hybrids between *M. m. musculus*^{PWD} × *M. m. domesticus*^{WSB} (White *et al.* 2011) to set thresholds for infertility in the F_2 males. For several phenotypes, a percentage of males fell within the sterile range (relative right testis weight, 22%; sperm density, 9.3%; proximal bent tail, 9.9%; distal bent tail, 17.3%; and amorphous sperm head, 8.0%), highlighting the importance of recessive factors contributing to hybrid male sterility. We also found high broad-sense heritabilities for each of these phenotypes (relative right testis weight, 0.837; sperm density, 0.768; seminiferous tubule area, 0.590; proximal bent tail, 0.927; distal bent tail, 0.884; headless/tailless sperm, 0.866; amorphous sperm head, 0.951; and total sperm abnormalities, 0.921), verifying that a large proportion of the phenotypic variance was due to genetic differences. Broad-sense heritability was not calculated for the principal component scores of sperm head morphology because the variance from the F_2's is not directly comparable to the variance among the parents and F_1's.

The majority of variation in sperm head morphology among the F_2 males was captured by two principal component scores. Principal component one (PC1) explained the curvature of the apical hook on the sperm head (PC1; 52.11% of the phenotypic variance; Figure 1B), whereas principal component two (PC2) accounted for an overall change in sperm head width (PC2; 25.91% of the phenotypic variance; Figure 1B). Similar to what was observed in sterile (*M. m. musculus*^{PWD} × *M. m. domesticus*^{WSB}) F_1 male hybrids (White *et al.* 2011), lower values of PC1 were associated with large reductions of the apical sperm head hook.

Most phenotypes were significantly correlated (Table 2), suggesting the presence of common genetic factors. Two phenotypes captured specific abnormalities in spermatogenesis that were largely independent of other hybrid sterility traits. Sperm head morphology PC2 was only negatively correlated with headless/tailless sperm (Table 2). In this case, higher proportions of headless/tailless sperm were associated with thinner sperm heads. The residual trait score of seminiferous tubule area was only negatively correlated with amorphous sperm heads (Table 2).

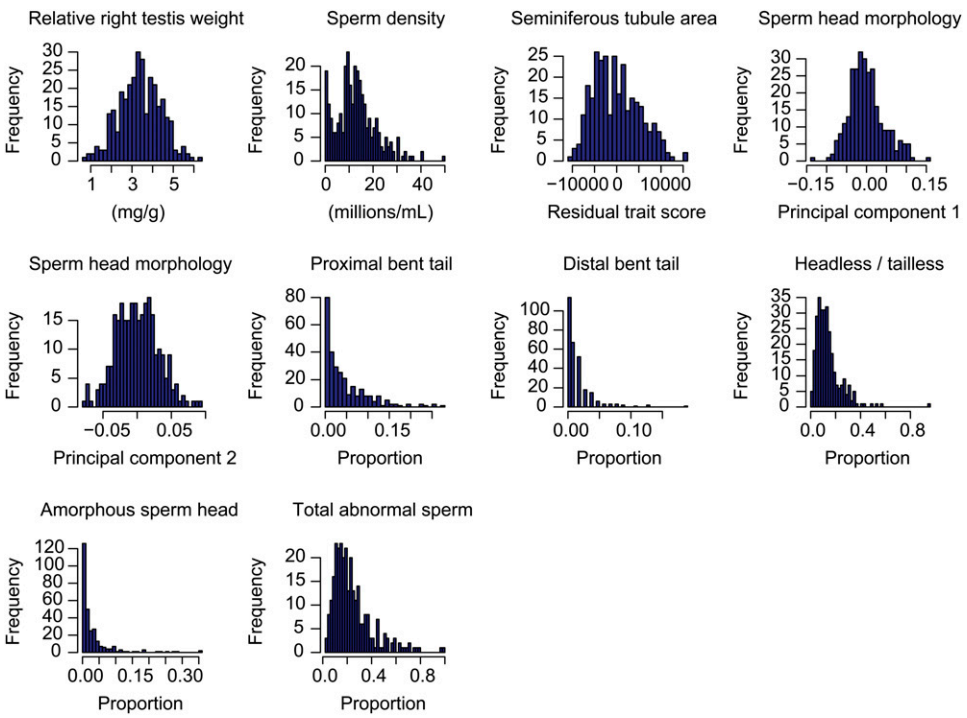

Figure 2 F_2 phenotype distributions from *M. m. castaneus*^{CAST} × *M. m. domesticus*^{WSB} intercross. Seminiferous tubule area is the residual trait score of tubule area regressed on testis weight.

Table 2 Spearman's rank correlation coefficients between hybrid sterility phenotypes

	Relative right testis	Sperm density	Sperm head PC1	Sperm head PC2	Semin. tubule area[a]	Prox. bent tail	Dist. bent tail	Headless /tailless	Amorph. head	Total abnormal sperm
Rel. right testis weight		**0.51**	**0.24**	0.01	0.02	**−0.31**	**−0.30**	**−0.29**	**−0.35**	**−0.42**
Sperm density	<0.001		**0.35**	−0.06	0.05	**−0.34**	**−0.20**	**−0.26**	**−0.47**	**−0.42**
Sperm head PC1	<0.001	<0.001		0	0.05	**−0.26**	**−0.15**	**−0.28**	**−0.38**	**−0.38**
Sperm head PC2	0.911	0.357	1		−0.04	−0.10	−0.10	**−0.14**	−0.001	−0.09
Semin. tubule area[a]	0.699	0.422	0.365	0.491		0.03	−0.05	0.09	**−0.17**	0.01
Prox. bent tail	<0.001	<0.001	<0.001	0.100	0.641		**0.25**	**0.25**	**0.31**	**0.62**
Dist. bent tail	<0.001	0.001	0.011	0.100	0.391	<0.001		**0.12**	**0.21**	**0.38**
Headless/tailless	<0.001	<0.001	<0.001	0.018	0.156	<0.001	0.050		**0.32**	**0.81**
Amorphous head	<0.001	<0.001	<0.001	0.992	0.004	<0.001	<0.001	<0.001		**0.58**
Total abnormal sperm	<0.001	<0.001	<0.001	0.123	0.826	<0.001	<0.001	<0.001	<0.001	

Upper diagonal, Spearman's rho with significant correlations in bold; lower diagonal, *P* values.
[a] Residual trait scores of seminiferous tubule area regressed on testis weight.

Figure 3 Single QTL scan for hybrid male sterility. The 1.5 LOD support intervals for QTL that exceed a genome-wide 5% significance threshold are shown (TW, relative right testis weight; SD, sperm density and sperm density binary; PC1, sperm head morphology PC1; STA, seminiferous tubule area; PBT, proximal bent tail; H/T, headless/tailless; ASH, amorphous sperm head; and TAS, total abnormal sperm). QTL mapping to the mitochondrion or Y chromosome are not shown.

Single QTL interval mapping

Using standard interval mapping, (Lander and Botstein 1989; Broman and Sen 2009), we found QTL associated with every phenotype except distal bent tail. For relative right testis weight, the strongest QTL was in the PAR, a narrow stretch of sequence homology on the distal end of the X and Y chromosomes (Figure 3; Tables 3 and 4; Supporting Information, Figure S1). We also detected testis weight QTL on chromosomes 2 and 4. The QTL in the PAR was consistent across multiple testis weight phenotypes (absolute right testis weight, relative right testis weight, and the residual trait scores of testis weight regressed on body weight); however, the QTL on chromosomes 2 and 4 dropped below a 5% significance threshold when mapped as absolute right testis weight and the residual trait scores of testis weight regressed on body weight (Table S1). For seminiferous tubule area, we found QTL on chromosomes 2 and 8, the distal end of the X chromosome, and within the PAR. The phenotypic distributions for other phenotypes exhibited strong skews from normality (Figure 2). We used transformations and alternative mapping methods for these phenotypes to assess the robustness of the results. Results were consistent across methodologies except for one phenotype (proximal bent tail), where the QTL dropped below a 5% significance threshold when mapped in a nonparametric framework (Table S2).

We detected several QTL associated with sperm density. When the entire phenotypic distribution was used for mapping, we detected a significant QTL on the distal end

Table 3 Single QTL mapping

Phenotype	Chr.	Position (cM)	LOD score[a]	Position (Mb)	1.5 LOD Int (Mb)	DD[b]	DC[b]	CC[b]
Rel. right testis weight	2	47.5	4.10	80.7	64.1–122.2	3.12 (±0.12)	3.40 (±0.08)	3.64 (±0.11)
	4	30	3.74	69.9	30.3–118.7	3.53 (±0.12)	3.53 (±0.09)	2.93 (±0.15)
Sperm density	X	58	3.75	141.7	87.3–162.9	14.68 (±0.68)	—	10.643 (±0.792)
Sperm density (binary)	X	6	3.13	21.8	10.2–48.6	0.98 (±0.03)	—	0.86 (±0.03)
Sperm head PC1[c]	2	96	4.35	177.5	149.1–179.0	−0.01 (±0.01)	−0.01 (±0.004)	0.02 (±0.01)
	X	56	3.79	137.9	10.2–162.9	−0.01 (±0.004)	—	0.01 (±0.004)
Sperm head PC2[c]	*M/Y*	0	11.07	—	—	0.02 (±0.003)	—	−0.01 (±0.002)
	X	16	10.85	41.3	21.8–100.7	−0.01 (±0.002)	—	0.01 (±0.003)
Semin. tubule area[d]	2	44	7.78	75.6	57.4–105.0	2401.97 (±661.27)	268.68 (±442.59)	−2637.73 (±643.27)
	8	60.6	4.53	125.0	112.7–130.8	1373.74 (±568.94)	266.27 (±404.28)	−2399.04 (±611.15)
	X	69.1	4.70	162.9	141.7–162.9	1174.16 (±388.86)	—	−1675.42 (±457.60)
Prox. bent tail[e]	X	60	3.33	145.5	93.9–162.9	0.19 (±0.01)	—	0.24 (±0.01)
Headless/tailless[e]	X	48	10.12	113.5	57.6–133.6	0.33 (±0.01)	—	0.44 (±0.02)
Amorph. sperm head[e]	2	86	4.95	169.1	133.7–177.5	0.13 (±0.01)	0.16 (±0.01)	0.21 (±0.01)
	9	2	8.13	14.4	3.1–29.8	0.16 (±0.01)	0.14 (±0.01)	0.23 (±0.01)
	X	40	3.53	93.9	45.1–162.9	0.14 (±0.01)	—	0.20 (±0.01)
Total abnormal sperm[e]	X	50	9.60	120.2	93.9–141.7	0.44 (±0.02)	—	0.59 (±0.01)

[a] All QTL are significant at a 5% significance threshold.
[b] Phenotype means of each genotype (±SE). D, *M. m. domesticus*^{WSB}; M, *M. m. castaneus*^{CAST}.
[c] Transformed to normal quantiles. Higher values of PC1 and PC2 are correlated with higher levels of sterility.
[d] Residual trait scores of seminiferous tubule area regressed on testis weight. Lower values are correlated with higher levels of sterility.
[e] Arcsine squareroot transformed.

of the X chromosome and within the PAR (Figure 2; Tables 3 and 4). Sperm density was converted to a binary character to account for the large number of males with near-zero sperm densities (Figure 2). We split the distribution into two bins by setting a threshold (1.5 millions/mL) that maximized the LOD score of the QTL on the X chromosome. When treated as a binary character, we detected a significant QTL at the proximal end of the X chromosome. We also analyzed sperm density with a two-part procedure, which uses two separate models to map the trait (Broman 2003; Broman and Sen 2009): a binary trait above and below a threshold (1.5 millions/mL) and a normal, quantitative character above the threshold. Consistent with what was observed with the binary model, the QTL on the proximal end of the X chromosome largely controlled high *vs.* low sperm density, whereas the QTL on the distal end of the X chromosome affected variation within the normal range of the distribution. The QTL within the PAR affected high *vs.* low sperm density and variation within the normal range of the distribution (Figure 4).

All abnormal sperm types (proximal bent tail, headless/tailless sperm, amorphous sperm heads, and total abnormal sperm) had QTL linked to the distal end of the X chromosome and within the PAR (Figure 3; Tables 3 and 4). In addition, amorphous sperm head was associated with two autosomal QTL on chromosomes 2 and 9. Proximal bent tail and amorphous sperm head had spikes at zero in their distributions, so we also applied a two-part model to differentiate the binary and quantitative portions of the traits (as described above). The effects of the X-linked QTL varied among phenotypes (Figure 4). For proximal bent tail, the QTL affected both the presence and absence of the trait as well as variation within the quantitative portion of the distribution. For amorphous sperm head, the X-linked QTL only contributed to variation within the quantitative range. Autosomal QTL had mixed effects, contributing to the presence of amorphous heads and variation within the normal range. The PAR QTL only contributed to variation within the normal range of the distributions.

Sperm head morphology PC1 and PC2 were associated with autosomal, X-linked, and PAR-linked QTL. Sperm head morphology PC1 was linked to chromosome 2, the distal end of chromosome X, and the PAR, whereas sperm head morphology PC2 was linked to the proximal end of chromosome X and the PAR (Figure 3; Tables 3 and 4). For PC2, we also found a strongly supported QTL linked to the mitochondrion or Y chromosome.

With the exception of the relative right testis weight QTL on chromosome 2 and sperm head morphology PC2 on the mitochondrion or Y chromosome, sterility was consistently associated with *M. m. castaneus*^{CAST} alleles (Table 3). On the autosomes, sterility connected to *M. m. castaneus*^{CAST} alleles spanned a range of dominance effects. On chromosome 2, there was evidence for several distinct effects. At the proximal end of chromosome 2, sterility was

Table 4 QTL linked to the pseudoautosomal region

Cross direction	Phenotype	LOD score[a]	DD[b]	DC[b]	CC[b]
Dom. × Cast.	Rel. right testis weight	6.20	3.57 (±0.26)	2.92 (±0.12)	3.92 (±0.13)
Cast. × Dom.	Rel. right testis weight	7.33	3.73 (±0.09)	3.62 (±0.24)	2.93 (±0.01)
	Sperm density	6.44	15.69 (±0.80)	17.02 (±2.16)	9.94 (±0.92)
	Sperm head PC1[c]	4.12	0.01 (±0.004)	0.02 (±0.01)	−0.02 (±0.01)
	Sperm head PC2[c]	3.14	0.002 (±0.003)	0.01 (±0.01)	0.02 (±0.003)
	Semin. tubule area[d]	10.64	1788.93 (±459.11)	4039.19 (±1240.40)	−2897.30 (±532.58)
	Prox. bent tail[e]	3.74	0.19 (±0.01)	0.19 (±0.03)	0.25 (±0.01)
	Headless/tailless[e]	5.26	0.34 (±0.01)	0.33 (±0.03)	0.42 (±0.01)
	Amorph. sperm head[e]	4.73	0.14 (±0.01)	0.12 (±0.03)	0.21 (±0.01)
	Total abnormal sperm[e]	7.98	0.44 (±0.02)	0.42 (±0.05)	0.59 (±0.02)

[a] Only QTL with a LOD score >3 are shown.
[b] Phenotype means of each genotype (±SE). D, *M. m. domesticus*^{WSB}; M, *M. m. castaneus*^{CAST}.
[c] Transformed to normal quantiles. Lower values of PC1 and PC2 are correlated with higher levels of sterility.
[d] Residual trait scores of seminiferous tubule area regressed on testis weight. Lower values are correlated with higher levels of sterility.
[e] Arcsine squareroot transformed.

associated with the *M. m. domesticus*^{WSB} allele for relative right testis weight and with the *M. m. castaneus*^{CAST} allele for seminiferous tubule area. At the distal end of chromosome 2, sterility was associated with the *M. m. castaneus*^{CAST} allele for sperm head morphology PC1.

Linkage to the pseudoautosomal region

The *M. m. castaneus*^{CAST} PAR is larger than the PAR in *M. m. domesticus*^{WSB} (M. A. White and B. A. Payseur, unpublished results). Markers within this extended region can be genotyped from the *M. m. castaneus*^{CAST} X chromosome and the PAR of the Y chromosome, but only from the *M. m. domesticus*^{WSB} X chromosome. Therefore, markers within this region exhibit segregation patterns that are specific to the direction of the intercross (Figure 5). To account for these different segregation patterns, we treated cross-direction as an additive covariate and performed single QTL interval mapping within the PAR. We found a strong QTL for relative right testis weight associated with the PAR in both directions of the intercross (Table 4). In the *M. m. domesticus*^{WSB} X chromosome × *M. m. castaneus*^{CAST} Y chromosome direction, the greatest reduction in testis weight occurred when the region was heterozygous (DC^{sterile} genotype in Table 4; Figure 5). In the *M. m. castaneus*^{CAST} X chromosome × *M. m. domesticus*^{WSB} Y chromosome direction, testis weight was only reduced when the PAR region was paired with a *M. m. domesticus* Y chromosome PAR (CC^{sterile} genotype in Table 4; Figure 5).

The DC^{sterile} and CC^{sterile} genotypes (*M. m. domesticus*^{WSB} X chromosome × *M. m. castaneus*^{CAST} Y chromosome direction and *M. m. castaneus*^{CAST} X chromosome × *M. m. domesticus*^{WSB} Y chromosome direction, respectively) contain a mixture of recombinant and nonrecombinant Y chromosomes (Figure 5). Although we could not distinguish the two with available markers, we estimated the fraction of each type of chromosome by comparing to the number of recombinant Y chromosomes in the DD and DC genotypes (*M. m. domesticus*^{WSB} X chromosome × *M. m. castaneus*^{CAST} Y chromosome direction and *M. m. castaneus*^{CAST} X chromosome × *M. m. domesticus*^{WSB} Y chromosome direction,

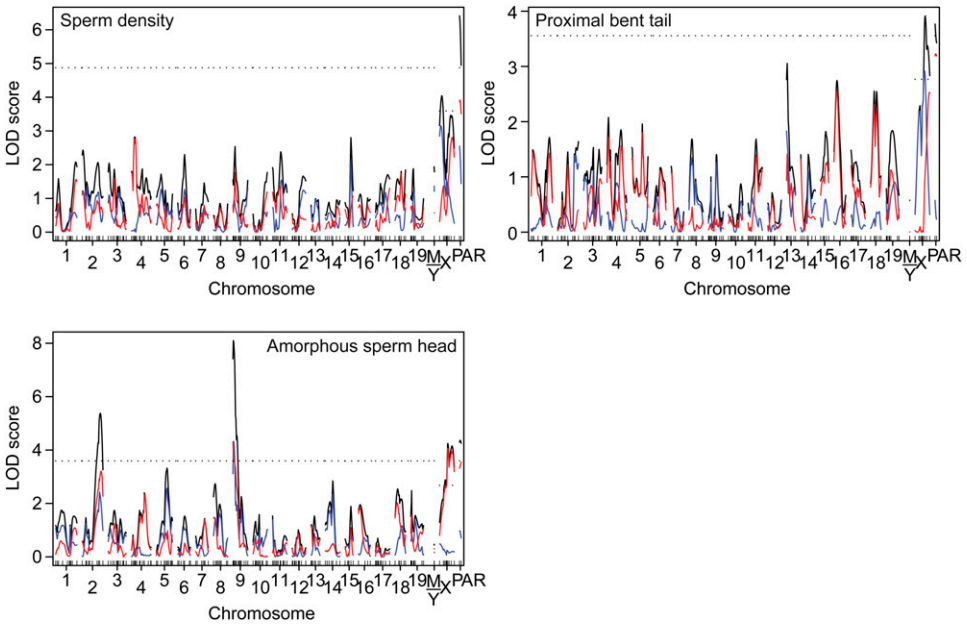

Figure 4 Single QTL scans with two-part models. The models evaluate support for QTL associations from the presence/absence of the trait (blue line), the normal portion of the distribution (red line), and the combined distribution (black line). Genome-wide significance thresholds are indicated by the dashed lines and were derived independently for the autosomes and the X chromosome from 1000 permutations of the combined distribution model (black line) (α = 0.05).

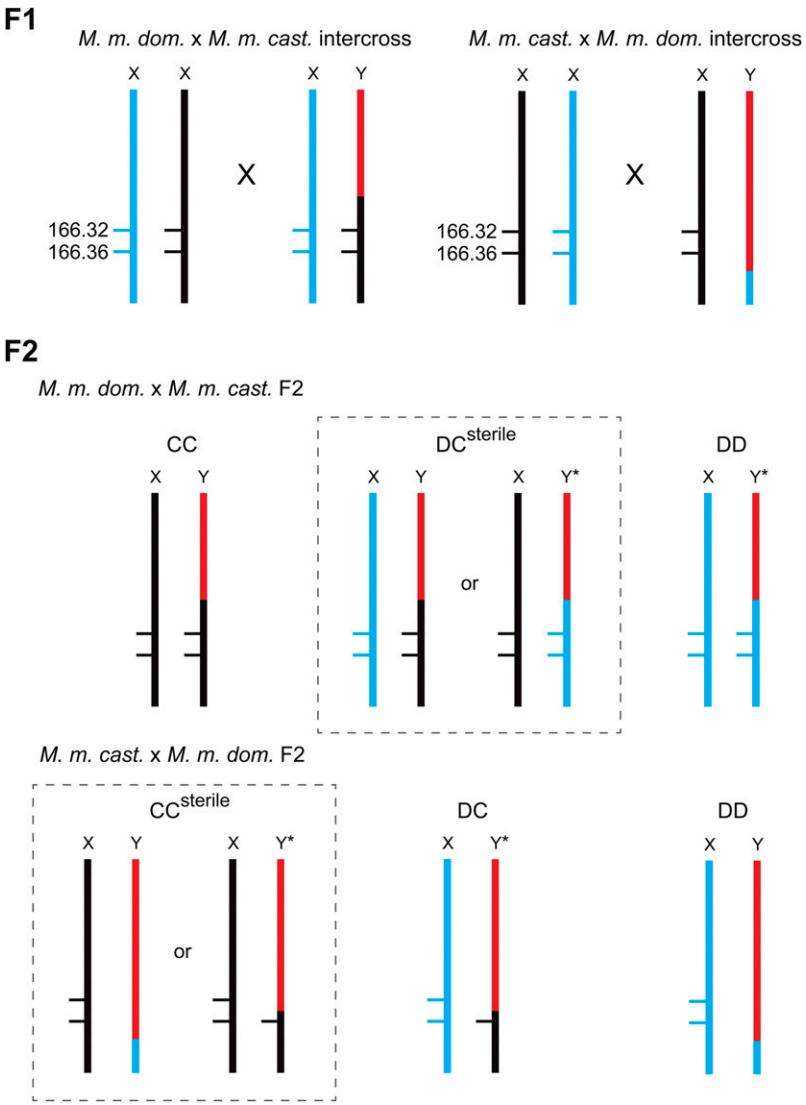

Figure 5 Pseudoautosomal region (PAR) SNP markers in F_1 and F_2 animals. Two markers (denoted by horizontal lines) are present within the Y chromosome PAR of *M. m. castaneus*^{CAST} but not within the Y chromosome PAR of *M. m. domesticus*^{WSB}. All genotypes from both intercross directions are shown. *M. m. domesticus*^{WSB} alleles are shown in blue and *M. m. castaneus*^{CAST} alleles are shown in black. The red region of the Y chromosome denotes sequence that is nonhomologous with the X chromosome. Sterile genotypes in F_2 males are shown in dashed boxes. Recombinant Y chromosomes have asterisks. We detected some recombinants between the *M. m. castaneus* X chromosome and the nonhomologous region of the *M. m. domesticus* Y chromosome, as indicated by the *M. m. castaneus* genotype present on the *M. m. domesticus* Y chromosome (lower cross).

respectively) (Figure 5). We found 11 males with a DD genotype and 15 males with a DC genotype. Because roughly equal numbers of recombinant Y chromosomes should be present in the DC^{sterile} and CC^{sterile} genotypes, we estimated that 76.6% (36 of 47 males) of the DC^{sterile} genotype was composed of a nonrecombinant *M. m. castaneus* Y chromosome paired with a *M. m. domesticus* X chromosome and 83.1% (74 of 89) of the CC^{sterile} genotype was composed of a nonrecombinant *M. m. domesticus* Y chromosome paired with a *M. m. castaneus* X chromosome. Both directions of the cross indicated that sterility is a consequence of heterozygosity, suggesting that mispairing of structurally different PARs might be involved.

Although heterozygosity in the PAR caused sterility in both directions of the cross, the phenotypic effects appeared to differ between directions of the intercross. The remainder of the phenotypes (sperm density, sperm head morphology PC1, sperm head morphology PC2, seminiferous tubule area, proximal bent tail, headless/tailless sperm, amorphous sperm head, and total abnormal sperm; Table 4) were only linked to the PAR in the *M. m. castaneus*^{CAST} × *M. m. domesticus*^{WSB} cross direction. In every case, the phenotypic means of genotypic classes matched the pattern observed for relative right testis weight, with reduced fertility in heterozygotes with the *M. m. domesticus*^{WSB} Y chromosome PAR.

Multiple QTL mapping

To look for additional QTL and epistatic interactions, we fit multiple QTL models. We first considered two-locus genotypic combinations. All mapping was conducted in a parametric framework. Using a genome-wide significance threshold of 5%, we detected pairs of QTL for relative right testis weight (2 and 4, 2 and PAR, 4 and PAR, M/Y and X, M/Y and PAR), seminiferous tubule area (2 and 2, 2 and 8, 2 and 10, 2 and X, 2 and PAR, 8 and 10, 8 and X, 8 and PAR, 10 and X, M/Y and X, X and PAR), sperm head morphology PC1 (2 and X, 2 and PAR, X and PAR), sperm head morphology PC2 (4 and X, 5 and PAR, M/Y and X, M/Y and PAR, X and X, X and PAR), and amorphous sperm head (2 and 9, 2 and X, 2 and PAR, 9 and X, 9 and PAR) (Table S3).

Table 5 Multiple QTL Mapping

Phenotype	Chr.	Position (cM)	LOD score[a]	Position (Mb)	1.5 LOD interval (Mb)	% Phen. Variance[b]	Additive[c]	Dominance[d]	Effect[e]
Rel. right testis weight	2	47.5	6.91	80.7	68.4–107.8	7.40	0.38 (±0.07)	0.17 (±0.10)	Dom. additive
	4	30	5.31	69.9	28.8–112.6	5.62	−0.35 (±0.08)	0.24 (±0.11)	Cast. recessive
	10	51	3.53	106.4	49.7–127.7	3.68	0.31 (±0.08)	0.02 (±0.11)	Dom. additive
	M/Y	0	7.45	—	—	8.01	−0.86 (±0.15)	—	Cast.
	PAR[f]	0	14.44	—	—	16.37	—	—	—
Sperm density	PAR[f]	0	5.59	—	—	8.12	—	—	—
Sperm head PC1[g]	2	97.7	4.28	179.0	142.3–179.0	6.23	0.01 (±0.003)	−0.007 (±0.005)	Cast. recessive
	PAR[f]	3	4.00	—	—	5.81	—	—	—
Sperm head PC2[g]	4	16.1	4.90	41.7	28.8–77.8	4.38	−0.01 (±0.002)	0.004 (±0.003)	Dom. additive
	5	12	3.80	32.5	9.01–148.4	3.37	−0.01 (±0.002)	−0.004 (±0.003)	Dom. recessive
	M/Y	0	17.31	—	—	17.13	−0.03 (±0.003)	—	Dom.
	X	12	6.33	33.5	10.2–49.5	5.72	0.01 (±0.002)	—	Cast.
	X	48	8.25	113.5	92.3–162.7	7.57	0.01 (±0.002)	—	Cast.
Semin. tubule area[h]	2	45	9.58	77.0	64.1–107.8	11.38	−2607.1 (±383.5)	155.3 (±582.6)	Cast. additive
	X	21	4.81	47.7	16.0–67.7	5.50	1280.8 (±269.9)	—	Dom.
	PAR[f]	0	10.71	—	—	12.85	—	—	—
Headless/tailless[i]	6	42	3.95	111.9	78.6–137.6	5.29	−0.05 (±0.01)	−0.03 (±0.02)	Dom. recessive
	X	42	10.30	97.3	52.0–133.6	14.53	0.06 (±0.01)	—	Cast.
Amorph. sperm head[i]	2	87	4.73	169.9	142.3–179.0	5.98	0.04 (±0.01)	0.001 (±0.01)	Cast. additive
	9	3	8.59	16.8	3.1–31.4	11.20	0.04 (±0.01)	−0.04 (±0.01)	Cast. recessive
	X	60	4.63	145.5	84.0–162.9	5.85	0.03 (±0.01)	—	Cast.
Total abnormal sperm[i]	X	48	9.33	113.5	92.3–151.3	13.90	0.08 (±0.01)	—	Cast.

[a] All QTL are significant at a 5% genome-wide significance threshold.
[b] Percentage of phenotypic variance explained by the QTL.
[c] Additive effect. Half the difference between the phenotype averages of the two homozygotes.
[d] Dominance deviation. Difference between the phenotype average of the heterozygotes and the midpoint of the phenotype averages of the two homozygotes.
[e] Subspecies allele associated with sterility and the effect of that allele. Dom., *M. m. domesticus*^{WSB}; Cast., *M. m. castaneus*^{CAST}.
[f] Effects of QTL in the PAR are not reported as they combine the effects across both cross directions.
[g] Transformed to normal quantiles.
[h] Residual trait scores of seminiferous tubule area regressed on testis weight.
[i] Arcsine squareroot transformed.

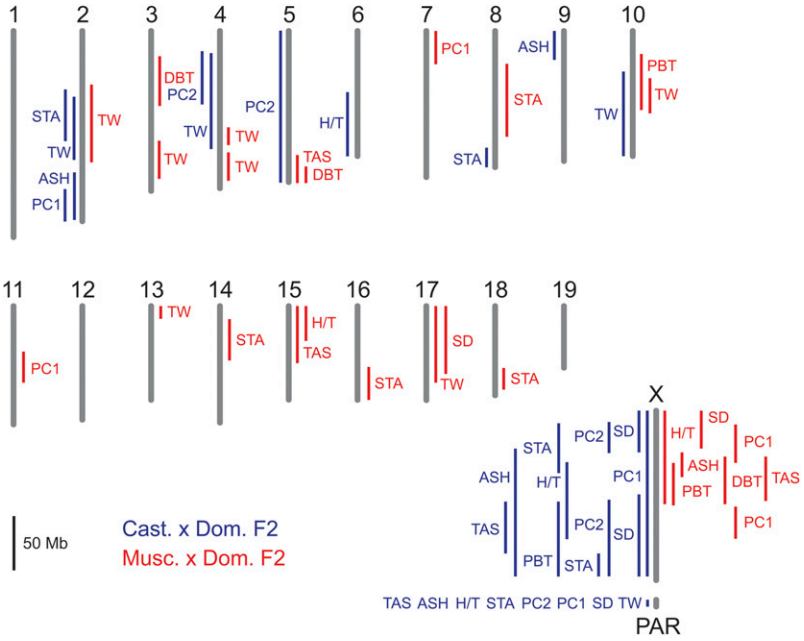

Figure 6 Comparison of hybrid sterility QTL from two intersubspecific crosses of house mice. The 1.5 LOD support intervals for QTL that exceed a genome-wide 5% significance threshold are shown from single QTL interval mapping and multiple QTL mapping (TW, relative right testis weight; SD, sperm density and sperm density binary; PC1, sperm head morphology PC1; STA, seminiferous tubule area; PBT, proximal bent tail; DBT, distal bent tail; H/T, headless/tailless; ASH, amorphous sperm head; and TAS, total abnormal sperm). Blue QTL are from the intercross between *M. m. castaneus*^{CAST} and *M. m. domesticus*^{WSB} and red QTL are from the intercross between *M. m. musculus*^{PWD} and *M. m. domesticus*^{WSB} (White *et al.* 2011). QTL that mapped to the mitochondrion or Y chromosome are not shown.

Phenotypic effects for most QTL pairs followed an additive mode; however, some phenotypes exhibited strong epistatic interactions between QTL on the distal end of the X chromosome and the mitochondrion or Y chromosome (Table S3). In these cases, a reduction in fertility was observed when the X chromosome was paired with the mitochondrion or Y chromosome of the other subspecies. This pairwise epistatic interaction mirrored the phenotypic patterns we observed for genotypic classes in the PAR, but with a lower LOD score. These results suggest that linkage to the distal end of the X chromosome and linkage to the PAR were driven by the same QTL.

We fit models that could incorporate more than two QTL using a forward/backward stepwise search algorithm. The percentage of phenotypic variance explained by these models varied among phenotypes (relative right testis weight, 30.84%; sperm density, 8.12%; sperm head morphology PC1, 12.55%; sperm head morphology PC2, 46.72%; seminiferous tubule area, 28.64%; headless/tailless, 19.19%; amorphous sperm head, 24.18%; and total abnormal sperm, 13.90%). Most QTL identified from two-locus QTL mapping were recovered by these analyses (Table 5). Multiple QTL mapping detected autosomal QTL that were missed by single QTL analyses, including loci at which the *M. m. domesticus*^{WSB} allele was associated with sterility (relative right testis weight, chromosome 10; sperm head morphology PC2, chromosomes 4 and 5; seminiferous tubule area, chromosome X; and headless/tailless, chromosome 6) (Table 5).

Shared sterility QTL with M. m. musculus^{PWD} × M. m. domesticus^{WSB} hybrids

Our previous identification of QTL for the same phenotypes in a similarly sized intercross between *M. m. musculus*^{PWD} and *M. m. domesticus*^{WSB} (White *et al.* 2011) allows a direct comparison of the genetic architecture of hybrid male sterility in two subspecies pairs. Statistical methods are available that map QTL shared in multiple crosses (Lyons *et al.* 2004), but they are not designed for epistatic QTL, including hybrid incompatibilities. To begin to characterize similarity in the genetic architecture of hybrid male sterility between subspecies pairs, we counted QTL with overlapping 1.5 LOD intervals. Three autosomal QTL intervals (chromosomes 2, 4, and 10) and several intervals on chromosome X overlapped between the two studies (Figure 6). The *M. m. domesticus*^{WSB} allele at chromosomes 2 and 10 reduced testis weight in both crosses. All other shared QTL were associated with the *M. m. musculus*^{PWD} or *M. m. castaneus*^{CAST} alleles. To determine whether the number of overlapping autosomal QTL was more than expected by chance, we permuted the *M. m. castaneus*^{CAST} × *M. m. domesticus*^{WSB} QTL and counted QTL that overlapped with QTL found in the *M. m. musculus*^{PWD} × *M. m. domesticus*^{WSB} intercross. Three or more shared QTL were observed in a large fraction of the 10,000 permutations ($P = 0.698$), suggesting that the observed overlap was within expectations under chance alone. Although this test ignores variation in marker density across the genome, the results reinforce the notion that few QTL are shared between the two crosses.

Discussion

The role of differences in fertility between M. m. domesticus^{WSB} and M. m. castaneus^{CAST}

Loci on the autosomes, the X chromosome, and in the PAR confer hybrid male sterility between *M. m. domesticus*^{WSB} and *M. m. castaneus*^{CAST}. These QTL may fall into two broad categories. First, they could reflect hybrid incompatibilities that are not present in the parental strains. Second, QTL

could be responsible for phenotypic differences between strains, but not hybrid dysfunction. QTL in the first category are connected to the speciation process; those belonging to the second category are not. The conflation of these QTL classes is a challenge faced by all mapping studies that involve crosses between reproductively isolated groups. In our study, the subfertility of *M. m. castaneus*^{CAST} raises the likely possibility that some QTL cause differences in fertility between the parental strains, but are not responsible for reproductive barriers between *M. m. castaneus* and *M. m. domesticus*.

The designation of individual QTL as hybrid incompatibilities or loci responsible for fertility differences among these strains will require additional studies. The Dobzhansky–Muller model predicts that heterosubspecific combinations of alleles at multiple loci interact to reduce fertility. The epistatic interactions between the distal end of the X chromosome and the Y chromosome or mitochondrial genome fit this prediction, but most QTL showed little evidence for epistasis. Statistical power to identify interacting QTL is limited in crosses of this size because the number of mice with the sterile multilocus genotype is small (epistasis can still generate marginal effects, allowing these loci to be detected as individual QTL). QTL mapping in larger crosses would help determine whether the QTL we detected represent hybrid incompatibilities. To conserve power, such studies could involve targeted genomic scans for epistasis involving the QTL reported here. Still, several pieces of evidence indicate that reproductive variation among F_2's reflects hybrid incompatibilities segregating in our intercross. First, the proximal bent tail sterility phenotype, which was prominent among F_2's, was largely absent from both parental strains. The elevated frequency of this phenotype in the F_2 generation (but not the F_1) requires epistasis involving recessive alleles. Second, *M. m. domesticus*^{WSB} alleles were associated with sterility at QTL for multiple phenotypes. Because *M. m. domesticus*^{WSB} males exhibited higher levels of fertility for every phenotype, these QTL require interactions with the *M. m. castaneus*^{CAST} genome to cause sterility in F_2's. Third, we detected significantly higher frequencies of apoptotic cells in the seminiferous tubules of F_1 hybrids than in the parental strains and an increase of unpaired X and Y chromosomes during meiosis, indicating dominant interactions between the parental genomes. Finally, the QTL with the strongest and most widespread effects on sterility (in the PAR) only reduced fertility when heterozygous, limiting its effects to hybrid mice.

F_1 hybrid male sterility

F_1 hybrids produced large numbers of F_2 progeny in both cross directions. F_1 fertility has been repeatedly observed in crosses between classical inbred mouse strains (largely of *M. m. domesticus* origin) and wild-caught (Anunciado *et al.* 2000; Ishikawa *et al.* 2000) or wild-derived inbred strains of *M. m. castaneus* (*e.g.*, Janaswami *et al.* 1997; Lyons *et al.* 2003, 2004; Yi *et al.* 2006), matching our observations. One contributor to this fertility could be introgression of small pieces of classical inbred strain genomes into the genome of *M. m. castaneus*^{CAST} (Yang *et al.* 2011). Nevertheless, we recovered developmental signs of abnormal spermatogenesis in the F_1 hybrids, including higher levels of apoptosis and a large frequency of spermatocytes carrying unpaired X and Y chromosomes at meiosis. One candidate for abnormal spermatogenesis in the F_1 hybrids between *M. m. castaneus*^{CAST} and *M. m. domesticus*^{WSB} is the PAR. Sterility was associated with a heterozygous PAR in the F_2 population, and the PAR was heterozygous in all F_1 males. The PAR has been previously linked to meiotic arrest and F_1 sterility in crosses between *Mus spretus* and C57BL/6J (Guénet *et al.* 1990; Matsuda *et al.* 1991, 1992; Hale *et al.* 1993).

Although F_1 hybrids between *M. m. castaneus*^{CAST} and *M. m. domesticus*^{WSB} were largely fertile, this may not be representative of the entire *M. m. castaneus* lineage. Fertility in F_1 hybrids has only been evaluated in a handful of inbred and wild representatives of *M. m. castaneus*, and F_1 hybrid male sterility is known to be polymorphic among strains of *M. m. musculus* and *M. m. domesticus* (Vyskočilová *et al.* 2005, 2009; Good *et al.* 2008b; Piálek *et al.* 2008). Furthermore, inbreeding depression in the parental strains might mask reduced fertility in the F_1's.

The inbred strains used in this study exhibit similar testis weights to wild populations of *M. m. castaneus* (Matsuda *et al.* 1982) and *M. m. domesticus* (Turner *et al.* 2012), arguing against severe effects of inbreeding depression. However, the other fertility phenotypes will need to be examined in outbred parental controls to determine whether F_1 hybrids between these subspecies are subfertile.

F_2 hybrid male sterility

A substantial fraction of F_2 males exhibited phenotypes that previously have been connected with sterility. High levels of abnormal sperm (Kawai *et al.* 2006) and strong reductions in the apical sperm hook (Immler *et al.* 2007; Firman and Simmons 2009) are negatively correlated with fertilization success in rodents; severely amorphous sperm heads are unable to fertilize ova (Krzanowska and Lorenc 1983; Oka *et al.* 2007; Styrna 2008). Furthermore, abnormal sperm head shapes often arise from aneuploidies during meiosis (Prisant *et al.* 2007; Perrin *et al.* 2008). All sterility phenotypes observed in F_1 and F_2 hybrids between *M. m. musculus*^{PWD} and *M. m. domesticus*^{WSB} except distal bent tail (White *et al.* 2011) were also observed in F_2 hybrids between *M. m. castaneus*^{CAST} and *M. m. domesticus*^{WSB}, indicating that these measures capture disruptions in spermatogenesis across multiple subspecies of house mice.

Several QTL for hybrid male sterility overlapped with genomic regions known to affect male reproductive traits in house mice. The testis weight QTL found on chromosomes 4 and 10 colocalize with QTL mapped in crosses between two classical inbred strains (Le Roy *et al.* 2001; Bolor *et al.* 2006) and in crosses between *M. m. musculus*^{PWD} and *M. m. domesticus*^{WSB} (White *et al.* 2011). The identification of this QTL in

multiple intra- and intersubspecific crosses suggests that it controls normal variation in testis weight in house mice. Sperm density (treated as a binary trait) maps to the proximal end of the X chromosome; this region reduces sperm density when introgressed from *M. m. musculus* into *M. m. domesticus* (Good *et al.* 2008a). The possibility that sperm head morphology PC2 and relative right testis weight map to the Y chromosome (they might instead be linked to mtDNA) agrees with previous results from crosses between classical inbred strains (Krzanowska 1969; Styrna *et al.* 1991a,b and 2002). Additionally, chromosome substitution strains that carried the middle or distal regions of chromosome 2 or the middle region of chromosome 6 from *M. m. castaneus*^{CAST} on the genomic background of a classical inbred strain suffered severe drops in fecundity (Davis *et al.* 2007).

We did not detect linkage to the region on chromosome 17 that harbors *Prdm9*, the only gene known to cause hybrid sterility in vertebrates (identified in crosses between *M. m. musculus* and a classical inbred strain (Forejt and Iványi 1974; Forejt 1996; Mihola *et al.* 2009). Divergence in the number of zinc fingers in the PRDM9 protein (Mihola *et al.* 2009) has been proposed as a mechanism for hybrid sterility; this divergence may disrupt the protein's ability to methylate histones (Oliver *et al.* 2009). However, heterozygosity in this region is not sufficient to cause sterility and requires additional interacting factors (Forejt 1996). Both *M. m. musculus*^{PWD} × *M. m. domesticus*^{WSB} and *M. m. castaneus*^{CAST} × *M. m. domesticus*^{WSB} crosses produce mice that are heterozygous for the number of zinc finger repeats (Parvanov *et al.* 2010), but only the *M. m. musculus*^{PWD} × *M. m. domesticus*^{WSB} cross yielded QTL in the *Prdm9* region (White *et al.* 2011). The role of *Prdm9* in house mouse speciation might be limited to hybrid male sterility between *M. m. musculus* and *M. m. domesticus*. A more detailed examination of abnormal spermatogenesis in *M. m. castaneus/M. m. domesticus* F_2 males will reveal whether spermatogenesis arrests during late pachytene, where *Prdm9* has its primary effect on hybrid sterility (Forejt and Iványi 1974; Yoshiki *et al.* 1993).

Comparing the genetic architecture of hybrid male sterility in two subspecies pairs

Our genetic studies of hybrid male sterility in *M. m. domesticus*^{WSB} - *M. m. musculus*^{PWD} (White *et al.* 2011) and *M. m. domesticus*^{WSB} - *M. m. castaneus*^{CAST} revealed a subset of QTL that overlap between the two subspecies pairs. Some of these QTL may correspond with those identified in previous studies of hybrid male sterility in house mice. As in our study, sperm density and abnormal sperm morphology have been linked to the proximal end of the X chromosome in crosses between *M. m. molossinus* and *M. m. domesticus* (Oka *et al.* 2004) and in crosses between *M. m. musculus* and *M. m. domesticus* (Storchová *et al.* 2004; Good *et al.* 2008a; White *et al.* 2011). These QTL may have a common evolutionary origin. Fine-scale mapping will be necessary to distinguish whether these QTL reflect the same underlying mutation(s).

Combining results from single and multiple QTL analyses (and counting loci that contribute to multiple phenotypes once), we found eight autosomal QTL that contribute to hybrid male sterility between *M. m. castaneus*^{CAST} × *M. m. domesticus*^{WSB}. In comparison, we detected 16 autosomal QTL in crosses between *M. m. domesticus*^{WSB} and *M. m. musculus*^{PWD} (White *et al.* 2011). Because our two studies used a common strain (*M. m. domesticus*^{WSB}), measured the same phenotypes, genotyped a shared set of SNP markers, and featured similar sample sizes, these studies offered comparable power to detect QTL. As a result, we conclude that the larger number of autosomal QTL in *M. m. domesticus*^{WSB} × *M. m. musculus*^{PWD} reflects greater genetic complexity of hybrid male sterility between *M. m. musculus* and *M. m. domesticus* than between *M. m. castaneus* and *M. m. domesticus*, despite similar divergence times.

Most of the autosomal QTL we identified in either study (18 out of 21) were not shared among subspecies pairs. This result agrees with the phylogenetic history of house mice. High levels of phylogenetic discordance among gene trees indicate that the ancestor of *M. m. musculus* and *M. m. castaneus* diverged rapidly from the *M. m. domesticus* lineage (Tucker *et al.* 1989; Prager *et al.* 1996, 1998; Lundrigan *et al.* 2002; Goios *et al.* 2007; Geraldes *et al.* 2008; Liu *et al.* 2008; White *et al.* 2009; Keane *et al.* 2011). The short internal branch leading from the root to the most recent common ancestor of *M. m. musculus* and *M. m. castaneus* provided little time for derived-derived incompatibilities (Orr 1995) to evolve. As a result, shared incompatibilities are more likely to have arisen along the *M. m. domesticus* lineage as ancestral-derived incompatibilities. Therefore, most incompatibilities should be unshared between these two subspecies pairs because unshared mutations could have accumulated on both the *M. m. musculus* and *M. m. castaneus* branches. Genetic mapping of hybrid male sterility between the third subspecies pair, *M. m. castaneus* and *M. m. musculus*, will assist with assigning incompatibilities to the phylogeny.

Hybrid male sterility and the PAR

Heterozygosity in the PAR was strongly associated with most hybrid sterility measures. The PAR is a small region of sequence homology between the X and Y chromosomes, which is restricted to the distal 700 kb of the X chromosome in house mice (Burgoyne 1982; Palmer *et al.* 1997; Perry *et al.* 2001). During each male meiosis, an obligate crossover in this small region helps ensure accurate pairing and segregation of the sex chromosomes (Keitges *et al.* 1985; Rouyer *et al.* 1986; Soriano *et al.* 1987). Disruptions in pairing (Burgoyne *et al.* 1992; Mohandas *et al.* 1992) or reduced recombination (Shi *et al.* 2001) can result in aneuploidies or complete meiotic arrest. Consequently, subspecies divergence within the PAR could directly reduce male fertility.

Our results highlight several novel patterns of PAR-linked hybrid male sterility. This is the first example of PAR-linked

hybrid sterility among very recently diverged lineages. Hybrid male sterility between more divergent species, *Mus spretus* and *M. m. domesticus* (C57BL/6J) (She *et al.* 1990; Suzuki *et al.* 2004), has been mapped to the PAR (Guénet *et al.* 1990). In this species pair, sterility was also limited to heterozygotes (Matsuda *et al.* 1991; Hale *et al.* 1993), in which high levels of dissociation among the X and Y chromosomes triggered meiotic arrest (Matsuda *et al.* 1992; Oka *et al.* 2010). We observed high frequencies of spermatocytes carrying unpaired X and Y chromosomes at late pachytene in F_1 hybrids between *M. m. castaneus*^{CAST} and *M. m. domesticus*^{WSB}, an effect likely caused by intersubspecific differences in the PAR region. The increased sterility in F_2 hybrids may be attributed to epistatic interactions between a heterozygous PAR and homozygous (recessive) loci elsewhere in the genome.

Other crosses implicate the *M. m. castaneus*^{CAST} X chromosome as a source of incompatibilities. The *M. m. castaneus*^{CAST} X chromosome was underrepresented in the Collaborative Cross, a set of recombinant inbred lines resulting from crosses between eight strains (Collaborative Cross Consortium 2012). Because the founder strains were biased toward *M. m. domesticus* ancestry, selection against the *M. m. castaneus*^{CAST} X chromosome might have been driven by the PAR-associated hybrid sterility we document here.

Genetic characterization of PAR-linked hybrid male sterility

The high level of variation in hybrid male sterility we observed among heterozygous genotypes indicates that additional genetic factors contribute to PAR-linked hybrid sterility. Although the detailed mechanisms underlying X and Y pairing in the PAR remain unknown, evidence is beginning to indicate that unique mechanisms regulate recombination in this region. In house mice, the PAR harbors an exceptionally high number of double-strand break repair hotspots (Smagulova *et al.* 2011) and uses machinery to repair double-strand breaks that is distinct from the rest of the genome (Kauppi *et al.* 2011). A more detailed quantification of meiotic defects between *M. m. castaneus*^{CAST} and *M. m. domesticus*^{WSB} will enable mapping of loci that modify PAR-linked hybrid sterility between these subspecies, leading to the discovery of genes specific to X and Y pairing, recombination, and segregation during meiosis.

Several genetic tools exist in these subspecies to aid in fine mapping of genes associated with these traits. Numerous mutant mouse strains have been generated that harbor abnormalities in male reproductive phenotypes (reviewed in Matzuk and Lamb 2002, 2008). These resources provide an extensive list of candidate genes underlying QTL. Furthermore, the eight founder strains of the collaborative cross include *M. m. domesticus*^{WSB} and *M. m. castaneus*^{CAST} (Churchill *et al.* 2004). This inbred panel of mice should accelerate fine mapping of the hybrid sterility QTL identified here and our results will aid the interpretation of sterility patterns segregating in this larger cross.

Acknowledgments

We thank Jenny Wagner and John Bak for help measuring male sterility traits and Denise Schwahn for characterizing abnormal spermatogenesis in the testis histology samples. In addition, we thank Brian Steffy and Tim Wiltshire for conducting the genotyping, Karl Broman for assistance in the QTL mapping, Leslie Turner for useful discussions, Francois Bonhomme and Annie Orth for providing the CIM strain, and Michael Nachman and one anonymous reviewer for helpful comments on the manuscript. This research was funded by National Science Foundation grant DEB 0918000. M.A.W. was supported by an National Library of Medicine (NLM) training grant in Computation and Informatics in Biology and Medicine to the University of Wisconsin (NLM 2T15LM007359).

Literature Cited

Anunciado, R. V., T. Imamura, T. Ohno, F. Horio, and T. Namikawa, 2000 Developing a new model for non-insulin dependent diabetes mellitus (NIDDM) by using the Philippine wild mouse, Mus musculus castaneus. Exp. Anim. 49: 1–8.

Arends, D., P. Prins, R. C. Jansen, and K. W. Broman, 2010 R/qtl: high-throughput multiple QTL mapping. Bioinformatics 26: 2990–2992.

Barbash, D. A., 2011 Comment on "A test of the snowball theory for the rate of evolution of hybrid incompatibilities". Science 333: 1576.

Barbash, D. A., D. F. Siino, A. M. Tarone, and J. Roote, 2003 A rapidly evolving MYB-related protein causes species isolation in Drosophila. Proc. Natl. Acad. Sci. USA 100: 5302–5307.

Bayes, J. J., and H. S. Malik, 2009 Altered heterochromatin binding by a hybrid sterility protein in Drosophila sibling species. Science 326: 1538–1541.

Beck, J. A., S. Lloyd, M. Hafezparast, M. Lennon-Pierce, J. T. Eppig *et al.*, 2000 Genealogies of mouse inbred strains. Nat. Genet. 24: 23–25.

Bolor, H., N. Wakasui, W. Zhao, and A. Ishikawa, 2006 Detection of quantitative trait loci causing abnormal spermatogenesis and reduced testis weight in the small testis (Smt) mutant mouse. Exp Anim Tokyo 55: 97–108.

Bomblies, K., J. Lempe, P. Epple, N. Warthmann, C. Lanz *et al.*, 2007 Autoimmune response as a mechanism for a Dobzhansky-Muller-type incompatibility syndrome in plants. PLoS Biol. 5: e236.

Boursot, P., J.-C. Auffray, J. Britton-Davidian, and F. Bonhomme, 1993 The evolution of house mice. Annu. Rev. Ecol. Syst. 24: 119–152.

Boursot, P., W. Din, R. Anand, D. Darviche, B. Dod *et al.*, 1996 Origin and radiation of the house mouse: mitochondrial DNA phylogeny. J. Evol. Biol. 9: 391–415.

Brideau, N. J., H. A. Flores, J. Wang, S. Maheshwari, X. Wang *et al.*, 2006 Two Dobzhansky-Muller genes interact to cause hybrid lethality in Drosophila. Science 314: 1292–1295.

Britton-Davidian, J., F. Fel-Clair, J. Lopez, P. Alibert, and P. Boursot, 2005 Postzygotic isolation between the two European subspecies of the house mouse: estimates from fertility patterns in wild and laboratory-bred hybrids. Biol. J. Linn. Soc. Lond. 84: 379–393.

Broman, K., and S. Sen, 2009 *A Guide to QTL Mapping with R/qtl*, Springer-Verlag, New York.

Broman, K. W., 2003 Mapping quantitative trait loci in the case of a spike in the phenotype distribution. Genetics 163: 1169–1175.

Broman, K. W., L. B. Rowe, G. A. Churchill, and K. Paigen, 2002 Crossover interference in the mouse. Genetics 160: 1123–1131.

Broman, K. W., H. Wu, S. Sen, and G. A. Churchill, 2003 R/qtl: QTL mapping in experimental crosses. Bioinformatics 19: 889–890.

Burgoyne, P. S., 1982 Genetic homology and crossing over in the X and Y chromosomes of Mammals. Hum. Genet. 61: 85–90.

Burgoyne, P. S., S. K. Mahadevaiah, M. J. Sutcliffe, and S. J. Palmer, 1992 Fertility in mice requires X-Y pairing and a Y-chromosomal "spermiogenesis" gene mapping to the long arm. Cell 71: 391–398.

Butlin, R. K., 2005 Recombination and speciation. Mol. Ecol. 14: 2621–2635.

Carter, T. C., and D. S. Falconer, 1951 Stocks for detecting linkage in the mouse, and the theory of their design. J. Genet. 50: 307–323.

Cattani, M. V., and D. C. Presgraves, 2009 Genetics and lineage-specific evolution of a lethal hybrid incompatibility between *Drosophila mauritiana* and its sibling species. Genetics 181: 1545–1555.

Chen, J., J. Ding, Y. Ouyang, H. Du, J. Yang *et al.*, 2008 A triallelic system of S5 is a major regulator of the reproductive barrier and compatibility of indica-japonica hybrids in rice. Proc. Natl. Acad. Sci. USA 105: 11436–11441.

Churchill, G. A., D. C. Airey, H. Allayee, J. M. Angel, A. D. Attie *et al.*, 2004 The Collaborative Cross, a community resource for the genetic analysis of complex traits. Nat. Genet. 36: 1133–1137.

Collaborative Cross Consortium, 2012 The genome architecture of the collaborative cross mouse genetic reference population. Genetics 190: 389–401.

Coyne, J. A., and H. A. Orr, 1989 Patterns of speciation in Drosophila. Evolution 43: 362–381.

Davis, R. C., A. Jin, M. Rosales, S. Yu, X. Xia *et al.*, 2007 Genome-wide set of congenic mouse strains derived from CAST/Ei on a C57BL/6 background. Genomics 90: 306–313.

Dean, M. D., and M. W. Nachman, 2009 Faster fertilization rate in conspecific *vs.* heterospecific matings in house mice. Evolution 63: 20–28.

Dod, B., L. S. Jermin, P. Boursot, V. H. Chapman, J. T. Nielsen *et al.*, 1993 Counterselection on sex-chromosomes in the mus-musculus european hybrid zone. J. Evol. Biol. 6: 529–546.

Dod, B., C. Smadja, R. Karn, and P. Boursot, 2005 Testing for selection on the androgen-binding protein in the Danish mouse hybrid zone. Biol. J. Linn. Soc. Lond. 84: 447–459.

Dumont, B. L., and B. A. Payseur, 2011 Genetic analysis of genome-scale recombination rate evolution in house mice. PLoS Genet. 7: e1002116.

Dumont, B. L., M. A. White, B. Steffy, T. Wiltshire, and B. A. Payseur, 2011 Extensive recombination rate variation in the house mouse species complex inferred from genetic linkage maps. Genome Res. 21: 114–125.

Duvaux, L., K. Belkhir, M. Boulesteix, and P. Boursot, 2011 Isolation and gene flow: inferring the speciation history of European house mice. Mol. Ecol. 20: 5248–5264.

Feenstra, B., I. M. Skovgaard, and K. W. Broman, 2006 Mapping quantitative trait loci by an extension of the Haley-Knott regression method using estimating equations. Genetics 173: 2269–2282.

Ferree, P. M., and D. A. Barbash, 2009 Species-specific heterochromatin prevents mitotic chromosome segregation to cause hybrid lethality in Drosophila. PLoS Biol. 7: e1000234.

Firman, R. C., and L. W. Simmons, 2009 Sperm competition and the evolution of the sperm hook in house mice. J. Evol. Biol. 22: 2505–2511.

Forejt, J., 1996 Hybrid sterility in the mouse. Trends Genet. 12: 412–417.

Forejt, J., and P. Iványi, 1974 Genetic studies on male sterility of hybrids between laboratory and wild mice (Mus musculus L.). Genet. Res. 24: 189–206.

Frazer, K. A., E. Eskin, H. M. Kang, M. A. Bogue, D. A. Hinds *et al.*, 2007 A sequence-based variation map of 8.27 million SNPs in inbred mouse strains. Nature 448: 1050–1053.

Geraldes, A., P. Basset, B. Gibson, K. L. Smith, B. Harr *et al.*, 2008 Inferring the history of speciation in house mice from autosomal, X-linked, Y-linked and mitochondrial genes. Mol. Ecol. 17: 5349–5363.

Geraldes, A., P. Basset, K. L. Smith, and M. W. Nachman, 2011 Higher differentiation among subspecies of the house mouse (Mus musculus) in genomic regions with low recombination. Mol. Ecol. 20: 4722–4736.

Goios, A., L. Pereira, M. Bogue, V. Macaulay, and A. Amorim, 2007 mtDNA phylogeny and evolution of laboratory mouse strains. Genome Res. 17: 293–298.

Good, J. M., M. D. Dean, and M. W. Nachman, 2008a A complex genetic basis to X-linked hybrid male sterility between two species of house mice. Genetics 179: 2213–2228.

Good, J. M., M. A. Handel, and M. W. Nachman, 2008b Asymmetry and polymorphism of hybrid male sterility during the early stages of speciation in house mice. Evolution 62: 50–65.

Good, J. M., T. Giger, M. D. Dean, and M. W. Nachman, 2010 Widespread over-expression of the X chromosome in sterile F_1 hybrid mice. PLoS Genet. 6: e1001148.

Gregorová, S., P. Divina, R. Storchova, Z. Trachtulec, V. Fotopulosova *et al.*, 2008 Mouse consomic strains: exploiting genetic divergence between Mus m. musculus and Mus m. domesticus subspecies. Genome Res. 18: 509–515.

Guénet, J. L., C. Nagamine, D. Simon-Chazottes, X. Montagutelli, and F. Bonhomme, 1990 Hst-3: an X-linked hybrid sterility gene. Genet. Res. 56: 163–165.

Hale, D. W., L. L. Washburn, and E. Eicher, 1993 Meiotic abnormalities in hybrid mice of the C57BL/6J x Mus spretus cross suggest a cytogenetic basis for Haldane's rule of hybrid sterility. Cytogenet. Cell Genet. 63: 221–234.

Haley, C. S., and S. A. Knott, 1992 A simple regression method for mapping quantitative trait loci in line crosses using flanking markers. Heredity 69: 315–324.

Hollocher, H., and C.-I. Wu, 1996 The genetics of reproductive isolation in the Drosophila simulans clade: X *vs.* autosomal effects and male *vs.* female effects. Genetics 143: 1243–1255.

Immler, S., H. D. M. Moore, W. G. Breed, and T. R. Birkhead, 2007 By hook or by crook? Morphometry, competition and cooperation in rodent sperm. PLoS ONE 2: e170.

Ishikawa, A., Y. Matsuda, and T. Namikawa, 2000 Detection of quantitative trait loci for body weight at 10 weeks from Philippine wild mice. Mamm. Genome 11: 824–830.

Iványi, P., M. Vojtísková, P. Démant, and M. Micková, 1969 Genetic factors in the ninth linkage group influencing reproductive performance in male mice. Folia Biol. (Praha) 15: 401–421.

Janaswami, P. M., E. H. Birkenmeier, S. A. Cook, L. B. Rowe, R. T. Bronson *et al.*, 1997 Identification and genetic mapping of a new polycystic kidney disease on mouse chromosome 8. Genomics 40: 101–107.

Kao, K. C., K. Schwartz, and G. Sherlock, 2010 A genome-wide analysis reveals no nuclear Dobzhansky-Muller pairs of determinants of speciation between S. cerevisiae and S. paradoxus, but suggests more complex incompatibilities. PLoS Genet. 6: e1001038.

Kauppi, L., M. Barchi, F. Baudat, P. J. Romanienko, S. Keeney *et al.*, 2011 Distinct properties of the XY pseudoautosomal region crucial for male meiosis. Science 331: 916–920.

Kawai, Y., T. Hata, O. Suzuki, and J. Matsuda, 2006 The relationship between sperm morphology and in vitro fertilization ability in mice. J. Reprod. Dev. 52: 561–568.
Keane, T. M., L. Goodstadt, P. Danecek, M. A. White, K. Wong *et al.*, 2011 Mouse genomic variation and its effect on phenotypes and gene regulation. Nature 477: 289–294.
Keitges, E., M. Rivest, M. Siniscalco, and S. M. Gartler, 1985 X-linkage of steroid sulphatase in the mouse is evidence for a functional Y-linked allele. Nature 315: 226–227.
Krzanowska, H., 1969 Factor responsible for spermatozoan abnormality located on the Y chromosome in mice. Genet. Res. 13: 17–24.
Krzanowska, H., and E. Lorenc, 1983 Influence of egg investments on in-vitro penetration of mouse eggs by misshapen spermatozoa. J. Reprod. Fertil. 68: 57–62.
Lander, E. S., and D. Botstein, 1989 Mapping Mendelian factors underlying quantitative traits using RFLP linkage maps. Genetics 121: 185–199.
Laukaitis, C., E. Critser, and R. Karn, 1997 Salivary androgen-binding protein (ABP) mediates sexual isolation in Mus musculus. Evolution 51: 2000–2005.
Le Roy, I., S. Tordjman, D. Migliore-Samour, H. Degrelle, and P. Roubertoux, 2001 Genetic architecture of testis and seminal vesicle weights in mice. Genetics 158: 333–340.
Lee, H.-Y., J.-Y. Chou, L. Cheong, N.-H. Chang, S.-Y. Yang *et al.*, 2008 Incompatibility of nuclear and mitochondrial genomes causes hybrid sterility between two yeast species. Cell 135: 1065–1073.
Liu, Y.-H., A. Takahashi, T. Kitano, T. Koide, T. Shiroishi *et al.*, 2008 Mosaic genealogy of the Mus musculus genome revealed by 21 nuclear genes from its three subspecies. Genes Genet. Syst. 83: 77–88.
Long, Y., L. Zhao, B. Niu, J. Su, H. Wu *et al.*, 2008 Hybrid male sterility in rice controlled by interaction between divergent alleles of two adjacent genes. Proc. Natl. Acad. Sci. USA 105: 18871–18876.
Lundrigan, B. L., S. A. Jansa, and P. K. Tucker, 2002 Phylogenetic relationships in the genus mus, based on paternally, maternally, and biparentally inherited characters. Syst. Biol. 51: 410–431.
Lyons, M. A., H. Wittenburg, R. Li, K. A. Walsh, G. A. Churchill *et al.*, 2003 Quantitative trait loci that determine lipoprotein cholesterol levels in DBA/2J and CAST/Ei inbred mice. J. Lipid Res. 44: 953–967.
Lyons, M. A., H. Wittenburg, R. Li, K. A. Walsh, R. Korstanje *et al.*, 2004 Quantitative trait loci that determine lipoprotein cholesterol levels in an intercross of 129S1/SvImJ and CAST/Ei inbred mice. Physiol. Genomics 17: 60–68.
Macholán, M., P. Munclinger, M. Sugerková, P. Dufková, B. Bímová *et al.*, 2007 Genetic analysis of autosomal and X-linked markers across a mouse hybrid zone. Evolution 61: 746–771.
Macholán, M., S. J. E. Baird, P. Munclinger, P. Dufková, B. Bímová *et al.*, 2008 Genetic conflict outweighs heterogametic incompatibility in the mouse hybrid zone? BMC Evol. Biol. 8: 271.
Manichaikul, A., J. Y. Moon, S. Sen, B. S. Yandell, and K. W. Broman, 2009 A model selection approach for the identification of quantitative trait loci in experimental crosses, allowing epistasis. Genetics 181: 1077–1086.
Martin, N. H., and J. H. Willis, 2010 Geographical variation in postzygotic isolation and its genetic basis within and between two Mimulus species. Philos. Trans. R. Soc. Lond. B Biol. Sci. 365: 2469–2478.
Masly, J. P., and D. C. Presgraves, 2007 High-resolution genome-wide dissection of the two rules of speciation in Drosophila. PLoS Biol. 5: e243.
Matsuda, Y., H. T. Imai, K. Moriwaki, K. Kondo, and F. Bonhomme, 1982 X-Y chromosome dissociation in wild derived Mus musculus subspecies, laboratory mice, and their F1 hybrids. Cytogenet. Cell Genet. 34: 241–252.
Matsuda, Y., T. Hirobe, and V. M. Chapman, 1991 Genetic basis of X-Y chromosome dissociation and male sterility in interspecific hybrids. Proc. Natl. Acad. Sci. USA 88: 4850–4854.
Matsuda, Y., P. B. Moens, and V. M. Chapman, 1992 Deficiency of X and Y chromosomal pairing at meiotic prophase in spermatocytes of sterile interspecific hybrids between laboratory mice (Mus domesticus) and Mus spretus. Chromosoma 101: 483–492.
Matute, D. R., I. A. Butler, D. A. Turissini, and J. A. Coyne, 2010 A test of the snowball theory for the rate of evolution of hybrid incompatibilities. Science 329: 1518–1521.
Matzuk, M. M., and D. J. Lamb, 2002 Genetic dissection of mammalian fertility pathways. Nat. Cell Biol. 4: s41–s49.
Matzuk, M. M., and D. J. Lamb, 2008 The biology of infertility: research advances and clinical challenges. Nat. Med. 14: 1197–1213.
Mihola, O., Z. Trachtulec, C. Vlcek, J. C. Schimenti, and J. Forejt, 2009 A mouse speciation gene encodes a meiotic histone h3 methyltransferase. Science 323: 373–375.
Mohandas, T. K., R. M. Speed, M. B. Passage, P. H. Yen, A. C. Chandley *et al.*, 1992 Role of the pseudoautosomal region in sex-chromosome pairing during male meiosis: meiotic studies in a man with a deletion of distal Xp. Am. J. Hum. Genet. 51: 526–533.
Moulia, C., J. Aussel, and F. Bonhomme, 1991 Wormy mice in a hybrid zone: a genetic control of susceptibility to parasite infection. J. Evol. Biol. 4: 679–687.
Mouse Genome Sequencing Consortium, 2002 Initial sequencing and comparative analysis of the mouse genome. Nature 420: 520–562.
Moyle, L. C., 2007 Comparative genetics of potential prezygotic and postzygotic isolating barriers in a Lycopersicon species cross. J. Hered. 98: 123–135.
Moyle, L. C., and E. B. Graham, 2005 Genetics of hybrid incompatibility between *Lycopersicon esculentum* and *L. hirsutum*. Genetics 169: 355–373.
Moyle, L. C., and T. Nakazato, 2008 Comparative genetics of hybrid incompatibility: sterility in two Solanum species crosses. Genetics 179: 1437–1453.
Moyle, L. C., and T. Nakazato, 2010 Hybrid incompatibility "snowballs" between Solanum species. Science 329: 1521–1523.
Moyle, L. C., and B. A. Payseur, 2009 Reproductive isolation grows on trees. Trends Ecol. Evol. 24: 591–598.
Muller, H. J., 1942 Isolating mechanisms, evolution, and temperature. Biol. Symp. 6: 71–125.
Munclinger, P., E. Bozikova, M. Sugerkova, J. Pialek, and M. Macholan, 2002 Genetic variation in house mice (Mus, muridae, rodentia) from the Czech and Slovak republics. Folia Zool. (Brno) 51: 81–92.
Nachman, M. W., and B. A. Payseur, 2012 Recombination rate variation and speciation: theoretical predictions and empirical results from rabbits and mice. Philos. Trans. R Soc. B. Biol. Sci. 367: 409–421.
Noor, M., K. Grams, L. Bertucci, and J. Reiland, 2001 Chromosomal inversions and the reproductive isolation of species. Proc. Natl. Acad. Sci. USA 98: 12084–12088.
Oka, A., A. Mita, N. Sakurai-Yamatani, H. Yamamoto, N. Takagi *et al.*, 2004 Hybrid breakdown caused by substitution of the X chromosome between two mouse subspecies. Genetics 166: 913–924.
Oka, A., T. Aoto, Y. Totsuka, R. Takahashi, M. Ueda *et al.*, 2007 Disruption of genetic interaction between two autosomal regions and the X chromosome causes reproductive isolation between mouse strains derived from different subspecies. Genetics 175: 185–197.
Oka, A., A. Mita, Y. Takada, H. Koseki, and T. Shiroishi, 2010 Reproductive isolation in hybrid mice due to spermatogenesis defects at three meiotic stages. Genetics 186: 339–351.

Oliver, P. L., L. Goodstadt, J. J. Bayes, Z. Birtle, K. C. Roach *et al.*, 2009 Accelerated evolution of the Prdm9 speciation gene across diverse metazoan taxa. PLoS Genet. 5: e1000753.

Orr, H. A., 1995 The population genetics of speciation: the evolution of hybrid incompatibilities. Genetics 139: 1805–1813.

Orr, H. A., and M. Turelli, 2001 The evolution of postzygotic isolation: accumulating Dobzhansky-Muller incompatibilities. Evolution 55: 1085–1094.

Orth, A., T. Adama, W. Din, and F. Bonhomme, 1998 Natural hybridization of two subspecies of house mice, Musculus domesticus and Mus musculus castaneus, near Lake Casitas (California). Genome 41: 104–110.

Palmer, S., J. Perry, D. Kipling, and A. Ashworth, 1997 A gene spans the pseudoautosomal boundary in mice. Proc. Natl. Acad. Sci. USA 94: 12030–12035.

Parvanov, E. D., P. M. Petkov, and K. Paigen, 2010 Prdm9 controls activation of mammalian recombination hotspots. Science 327: 835.

Payseur, B., and M. Nachman, 2005 The genomics of speciation: investigating the molecular correlates of X chromosome introgression across the hybrid zone between Mus domesticus and Mus musculus. Biol. J. Linn. Soc. Lond. 84: 523–534.

Payseur, B. A., 2010 Using differential introgression in hybrid zones to identify genomic regions involved in speciation. Mol Ecol Resour 10: 806–820.

Payseur, B. A., J. G. Krenz, and M. W. Nachman, 2004 Differential patterns of introgression across the X chromosome in a hybrid zone between two species of house mice. Evolution 58: 2064–2078.

Perrin, A., F. Morel, L. Moy, D. Colleu, V. Amice *et al.*, 2008 Study of aneuploidy in large-headed, multiple-tailed spermatozoa: case report and review of the literature. Fertil. Steril. 90: 1201.e1–1201.e17.

Perry, J., S. Palmer, A. Gabriel, and A. Ashworth, 2001 A short pseudoautosomal region in laboratory mice. Genome Res. 11: 1826–1832.

Phadnis, N., and H. A. Orr, 2009 A single gene causes both male sterility and segregation distortion in Drosophila hybrids. Science 323: 376–379.

Piálek, J., M. Vyskočilová, B. Bímová, D. Havelková, J. Piálková *et al.*, 2008 Development of unique house mouse resources suitable for evolutionary studies of speciation. J. Hered. 99: 34–44.

Prager, E. M., H. Tichy, and R. D. Sage, 1996 Mitochondrial DNA sequence variation in the eastern house mouse, *Mus musculus*: comparison with other house mice and report of a 75-bp tandem repeat. Genetics 143: 427–446.

Prager, E. M., C. Orrego, and R. D. Sage, 1998 Genetic variation and phylogeography of central Asian and other house mice, including a major new mitochondrial lineage in Yemen. Genetics 150: 835–861.

Presgraves, D. C., 2003 A fine-scale genetic analysis of hybrid incompatibilities in Drosophila. Genetics 163: 955–972.

Presgraves, D. C., L. Balagopalan, S. M. Abmayr, and H. A. Orr, 2003 Adaptive evolution drives divergence of a hybrid inviability gene between two species of Drosophila. Nature 423: 715–719.

Prisant, N., D. Escalier, J.-C. Soufir, M. Morillon, D. Schoevaert *et al.*, 2007 Ultrastructural nuclear defects and increased chromosome aneuploidies in spermatozoa with elongated heads. Hum. Reprod. 22: 1052–1059.

Raufaste, N., A. Orth, K. Belkhir, D. Senet, C. Smadja *et al.*, 2005 Inferences of selection and migration in the Danish house mouse hybrid zone. Biol. J. Linn. Soc. Lond. 84: 593–616.

Rieseberg, L., 2001 Chromosomal rearrangements and speciation. Trends Ecol. Evol. 16: 351–358.

Rouyer, F., M. C. Simmler, C. Johnsson, G. Vergnaud, H. J. Cooke *et al.*, 1986 A gradient of sex linkage in the pseudoautosomal region of the human sex chromosomes. Nature 319: 291–295.

Russell, L. D., R. Ettlin, A. Sinha Hikin, and E. Clegg, 1990 *Histological and Histopathological Evaluation of the Testis*, Cache River Press, Clearwater, Florida.

Sage, R. D., W. Atchley, and E. Capanna, 1993 House mice as models in systematic biology. Syst. Biol. 42: 523–561.

Sage, R. D., D. Heyneman, K. C. Lim, and A. C. Wilson, 1986 Wormy mice in a hybrid zone. Nature 324: 60–63.

Salcedo, T., A. Geraldes, and M. W. Nachman, 2007 Nucleotide variation in wild and inbred mice. Genetics 177: 2277–2291.

Sawamura, K., and M. Yamamoto, 1997 Characterization of a reproductive isolation gene, zygotic hybrid rescue, of Drosophila melanogaster by using minichromosomes. Heredity 79: 97–103.

Searle, A. G., and C. V. Beechey, 1974 Sperm-count, egg-fertilization and dominant lethality after X-irradiation of mice. Mutat. Res. 22: 63–72.

She, J. X., F. Bonhomme, P. Boursot, L. Thaler, and F. Catzeflis, 1990 Molecular phylogenies in the genus Mus: comparative analysis of electrophoretic, scnDNA hybridization, and mtDNA RFLP data. Biol. J. Linn. Soc. Lond. 41: 83–103.

Shi, Q., E. Spriggs, L. L. Field, E. Ko, L. Barclay *et al.*, 2001 Single sperm typing demonstrates that reduced recombination is associated with the production of aneuploid 24,XY human sperm. Am. J. Med. Genet. 99: 34–38.

Smagulova, F., I. V. Gregoretti, K. Brick, P. Khil, R. D. Camerini-Otero *et al.*, 2011 Genome-wide analysis reveals novel molecular features of mouse recombination hotspots. Nature 472: 375–378.

Soriano, P., E. A. Keitges, D. F. Schorderet, K. Harbers, S. M. Gartler *et al.*, 1987 High rate of recombination and double crossovers in the mouse pseudoautosomal region during male meiosis. Proc. Natl. Acad. Sci. USA 84: 7218–7220.

Storchová, R., S. Gregorová, D. Buckiová, V. Kyselová, P. Divina *et al.*, 2004 Genetic analysis of X-linked hybrid sterility in the house mouse. Mamm. Genome 15: 515–524.

Styrna, J., 2008 Genetic control of gamete quality in the mouse–a tribute to Halina Krzanowska. Int. J. Dev. Biol. 52: 195–199.

Styrna, J., H. T. Imai, and K. Moriwaki, 1991a An increased level of sperm abnormalities in mice with a partial deletion of the Y chromosome. Genet. Res. 57: 195–199.

Styrna, J., J. Klag, and K. Moriwaki, 1991b Influence of partial deletion of the Y chromosome on mouse sperm phenotype. J. Reprod. Fertil. 92: 187–195.

Styrna, J., B. Bilińska, and H. Krzanowskaa, 2002 The effect of a partial Y chromosome deletion in B10.BR-Ydel mice on testis morphology, sperm quality and efficiency of fertilization. Reprod. Fertil. Dev. 14: 101–108.

Suzuki, H., T. Shimada, M. Terashima, K. Tsuchiya, and K. Aplin, 2004 Temporal, spatial, and ecological modes of evolution of Eurasian Mus based on mitochondrial and nuclear gene sequences. Mol. Phylogenet. Evol. 33: 626–646.

Sweigart, A. L., L. Fishman, and J. H. Willis, 2006 A simple genetic incompatibility causes hybrid male sterility in mimulus. Genetics 172: 2465–2479.

Tang, S., and D. C. Presgraves, 2009 Evolution of the Drosophila nuclear pore complex results in multiple hybrid incompatibilities. Science 323: 779–782.

Tao, Y., S. Chen, D. L. Hartl, and C. C. Laurie, 2003 Genetic dissection of hybrid incompatibilities between *Drosophila simulans* and *D. mauritiana*. I. Differential accumulation of hybrid male sterility effects on the X and autosomes. Genetics 164: 1383–1397.

Teeter, K. C., B. A. Payseur, L. W. Harris, M. A. Bakewell, L. M. Thibodeau *et al.*, 2008 Genome-wide patterns of gene flow across a house mouse hybrid zone. Genome Res. 18: 67–76.

Teeter, K. C., L. M. Thibodeau, Z. Gompert, C. A. Buerkle, M. W. Nachman *et al.*, 2010 The variable genomic architecture of isolation between hybridizing species of house mice. Evolution 64: 472–485.

Ting, C. T., S. C. Tsaur, M. L. Wu, and C.-I. Wu, 1998 A rapidly evolving homeobox at the site of a hybrid sterility gene. Science 282: 1501–1504.

True, J. R., B. S. Weir, and C. C. Laurie, 1996 A genome-wide survey of hybrid incompatibility factors by the introgression of marked segments of *Drosophila mauritiana* chromosomes into *Drosophila simulans*. Genetics 142: 819–837.

Tucker, P. K., B. Lee, and E. Eicher, 1989 Y-chromosome evolution in the subgenus *Mus* (Genus *Mus*). Genetics 122: 169–179.

Turelli, M., and H. A. Orr, 2000 Dominance, epistasis and the genetics of postzygotic isolation. Genetics 154: 1663–1679.

Turner, L. M., D. J. Schwahn, and B. Harr, 2012 Reduced male fertility is common but highly variable in form and severity in a natural house mouse hybrid zone. Evolution 66: 443–458.

Vanlerberghe, F., B. Dod, P. Boursot, M. Bellis, and F. Bonhomme, 1986 Absence of Y-chromosome introgression across the hybrid zone between Mus musculus domesticus and Mus musculus musculus. Genet. Res. 48: 191–197.

Vyskočilová, M., G. Pražanová, and J. Piálek, 2009 Polymorphism in hybrid male sterility in wild-derived Mus musculus musculus strains on proximal chromosome 17. Mamm. Genome 20: 83–91.

Vyskočilová, M., Z. Trachtulec, J. Forejt, and J. Pialek, 2005 Does geography matter in hybrid sterility in house mice? Biol. J. Linn. Soc. Lond. 84: 663–674.

White, M. A., C. Ané, C. N. Dewey, B. R. Larget, and B. A. Payseur, 2009 Fine-scale phylogenetic discordance across the house mouse genome. PLoS Genet. 5: e1000729.

White, M. A., B. Steffy, T. Wiltshire, and B. A. Payseur, 2011 Genetic dissection of a key reproductive barrier between nascent species of house mice. Genetics 189: 289–304.

Yang, H., T. A. Bell, G. A. Churchill, and F. Pardo-Manuel De Villena, 2007 On the subspecific origin of the laboratory mouse. Nat. Genet. 39: 1100–1107.

Yang, H., J. R. Wang, J. P. Didion, R. J. Buus, T. A. Bell *et al.*, 2011 Subspecific origin and haplotype diversity in the laboratory mouse. Nat. Genet. 43: 648–655.

Yi, N., D. K. Zinniel, K. Kim, E. J. Eisen, A. Bartolucci *et al.*, 2006 Bayesian analyses of multiple epistatic QTL models for body weight and body composition in mice. Genet. Res. 87: 45–60.

Yoshiki, A., K. Moriwaki, T. Sakakura, and M. Kusakabe, 1993 Histological studies on male-sterility of hybrids between laboratory and wild mouse strains. Dev. Growth Differ. 35: 271–281.

Communicating editor: D. Begun

GENETICS

Supporting Information
http://www.genetics.org/content/suppl/2012/05/02/genetics.112.140251.DC1

Genetics and Evolution of Hybrid Male Sterility in House Mice

Michael A. White, Maria Stubbings, Beth L. Dumont, and Bret A. Payseur

DOI: 10.1534/genetics.112.140251

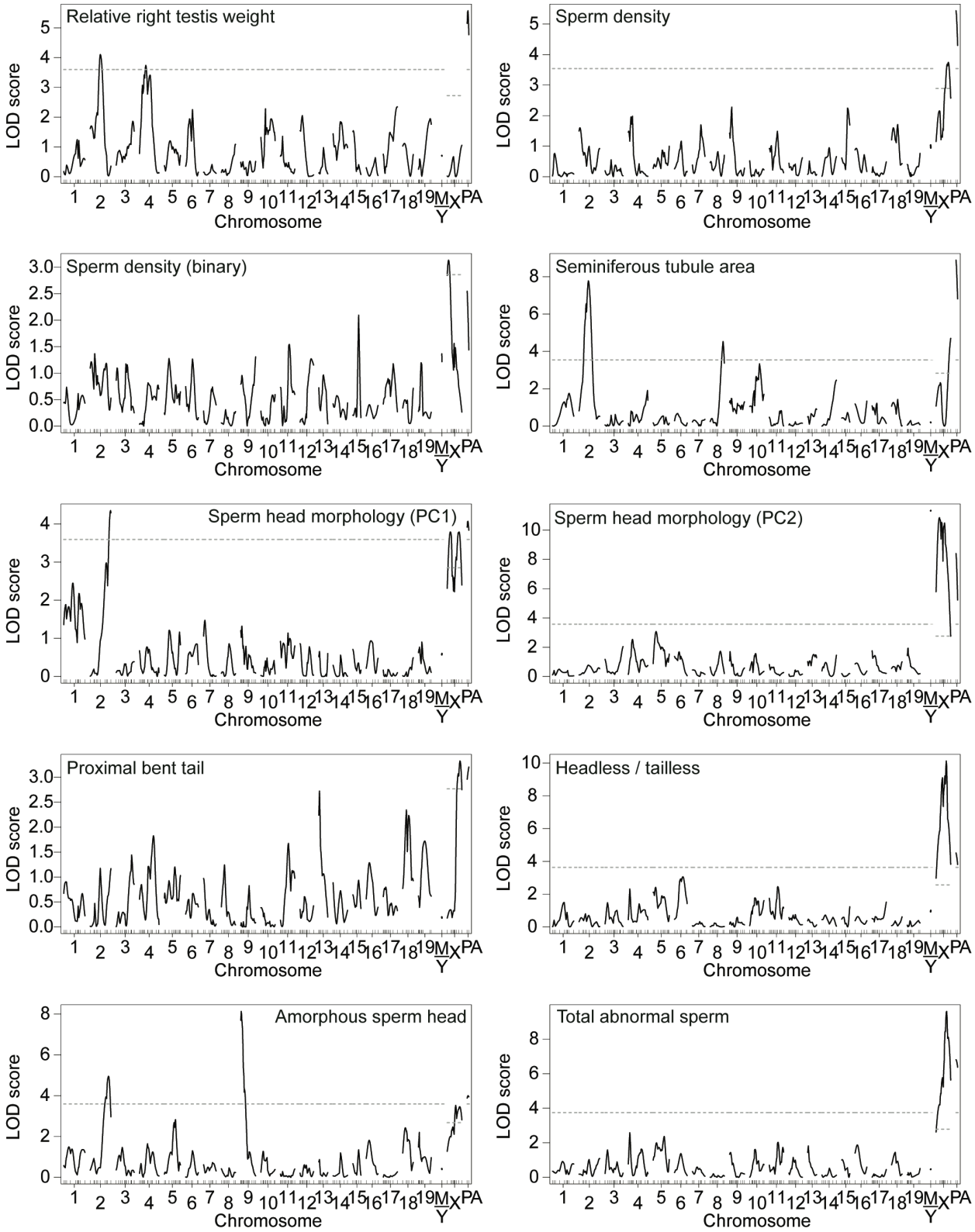

Figure S1 Single QTL mapping between *M. m. castaneus*^{CAST} and *M. m. domesticus*^{WSB}. Genome-wide significance thresholds are indicated by the dashed lines (alpha = 0.05). Seminiferous tubule area is the residual trait score of seminiferous tubule area regressed on testis weight. Sperm head morphology PC1 and PC2 is transformed to normal quantiles. All abnormal sperm types are arcsine square root transformed proportions. The mitochondrion and Y chromosome are depicted together (M/Y), as our crossing scheme cannot differentiate between the two. The pseudoautosomal region is indicated as PA

Table S1 Differences in QTL support between the three testis weight QTL. The significant QTL on chromosomes 6 and X for absolute testis weight are likely from an association between body weight and this phenotype (there are significant QTL for body weight on chromosomes 2, 6, and X; data not shown). The chromosome 2 QTL persists when body weight is accounted for through relative right testis weight. This suggests the QTL has an effect on both body weight and testis weight.

Phenotype	Chr.	Position (cM)	LOD score
Absolute right testis weight	2	47.5	1.49
	4	19.8	2.82
	6	32	3.87[a]
	X	62	2.90[a]
	PAR	-	6.11[a]
Relative right testis weight	2	47.5	4.11[a]
	4	30	3.74[a]
	6	32	2.25
	X	69.1	1.05
	PAR	-	5.58[a]
Residual trait scores[b]	2	47.5	2.66
	4	30	3.37
	6	32	3.23
	X	68	1.68
	PAR	-	6.09[a]

[a]LOD score is significant at a 5% significance threshold.
[b]Residual trait scores of testis weight regressed on body wekght.

Table S2 QTL that differed in significance between parametric and nonparametric single-QTL mapping.

Phenotype	Chr.	Position (cM)	Para. LOD score	Nonpara. LOD score
Proximal bent tail	X	60	3.329 [a]	2.573

[a]LOD score is significant at a 5% significance threshold.

Table S3 Two-dimensional, two-QTL scan.

Phenotype	Chrs.	Pos. 1 (cM)[a]	Pos. 2 (cM)[a]	Pos. 1 (Mb)[a]	Pos. 2 (Mb)[a]	LOD score (full)	LOD score (c.i.)[b]	LOD score (int.)	LOD score (add.)	LOD score (c.a)[c]
Rel. right testis weight	2 & 4	45	9	77.0	28.8	8.57	4.47	0.66	7.91[d]	3.81[d]
	2 & PAR	48	3	82.0	-	11.85[d]	6.25	1.32	10.53[d]	4.93[d]
	4 & PAR	33	3	77.8	-	10.79[d]	5.19	0.86	9.93[d]	4.33[d]
	M/Y & X	0	69	-	162.7	9.03[d]	7.98[d]	7.88[d]	1.15	0.10
	M/Y & PAR	0	3	-	-	14.27[d]	8.67[d]	3.08	11.19[d]	5.59[d]
Semin. tubule area[e]	2 & 2	57	87	107.8	169.9	14.85[d]	7.07[d]	4.43	10.42[d]	2.65
	2 & 8	45	60	77.0	124.4	12.96[d]	5.19	0.49	12.47[d]	4.70[d]
	2 & 10	45	48	77.0	102.4	11.50[d]	3.72	0.41	11.09[d]	3.32[d]
	2 & X	51	69	90.6	162.7	14.64[d]	6.87	2.02	12.62[d]	4.85[d]
	2 & PAR	45	0	77.0	-	19.40[d]	10.51[d]	2.26	17.14[d]	8.25[d]
	8 & 10	60	45	124.4	98.7	10.78[d]	6.31	3.17	7.61[d]	3.14[d]
	8 & X	60	69	124.4	162.7	8.87	4.17	0.62	8.25[d]	3.56[d]
	8 & PAR	60	0	124.4	-	12.49[d]	3.60	0.25	12.23[d]	3.35[d]
	10 & X	30	69	76.3	162.7	8.93[d]	4.23	0.73	8.19[d]	3.50[d]
	M/Y & X	0	69	-	162.7	11.09[d]	6.40	6.34[d]	4.76	0.06
	X & PAR	21	0	47.7	-	12.36[d]	3.48	0.12	12.24[d]	3.35[d]
Sperm head PC1[f]	2 & X	96	57	177.5	139.8	8.45	4.10	0.22	8.23[d]	3.88[d]
	2 & PAR	96	3	177.5	-	9.42[d]	5.07	1.05	8.37[d]	4.02[d]
	X & PAR	15	3	39.3	-	8.45	4.36	0.53	7.92[d]	3.84[d]
Sperm head PC2[f]	4 & X	18	27	45.0	60.4	14.64[d]	3.78	0.14	14.50[d]	3.65[d]
	5 & PAR	15	0	36.6	-	12.79[d]	4.39	0.57	12.21[d]	3.82[d]
	M/Y & X	0	27	-	60.4	26.40[d]	15.33[d]	0.42	25.99[d]	14.92[d]
	M/Y & PAR	0	0	-	-	15.45[d]	4.38	0.39	15.06[d]	3.99[d]
	X & X	15	42	39.3	97.3	15.25[d]	4.40	1.13	14.13[d]	3.27[d]
	X & PAR	15	0	39.3	-	20.08[d]	9.23[d]	0.17	19.91[d]	9.06[d]
Amorph. sperm head[g]	2 & 9	90	3	172.4	16.8	14.24[d]	6.11	1.62	12.62[d]	4.49[d]
	2 & X	84	60	167.3	145.5	8.85	3.95	0.14	8.71[d]	3.81[d]
	2 & PAR	90	0	172.4	-	11.55[d]	6.66	2.48	9.08[d]	4.18[d]
	9 & X	3	51	16.8	123.5	13.11[d]	4.98	0.59	12.52[d]	4.38[d]
	9 & PAR	3	3	16.8	-	12.73[d]	4.59	0.25	12.48[d]	4.35[d]

[a]Positions are estimated from the full model.
[b]LOD score supporting a conditional-interactive model (the support for a two locus model over a single locus model, allowing for the presence of an interaction).
[c]LOD score supporting a condional-additive model (the support for a two-locus model over a single locus model, assuming no interaction).
[d]Significant at a 5% threshold.
[e]Residual trait scores of seminiferous tubule area regressed on testis weight.
[f]Transformed to normal quantiles.
[g]Arcsine squareroot transformed.